DESIGN AND OPTIMIZATION OF A ONE-DEGREE-OF-FREEDOM EIGHT-BAR LEG MECHANISM FOR A WALKING MACHINE

By

Daniel Giesbrecht

A Thesis

Submitted to the Faculty of Graduate Studies

In Partial Fulfillment of the Requirements

For the Degree of

MASTER OF SCIENCE

*****

Department of Mechanical and Manufacturing Engineering

The University of Manitoba

Winnipeg, Manitoba

Abstract

The purpose of this study is to contribute to the area of mechanism design and optimization of a single-degree-of-freedom leg mechanism. The leg mechanism is considered to be very energy efficient especially when walking on rough terrains. Furthermore, the mechanism requires very simple controls since a single actuator is required to drive the leg. Previous work in this area had common focuses. First, the optimization was set up to change the length of each link directly. This can be time consuming since there is no structure other then changing the lengths and seeing how it affects the outcome. Second, a static analysis was used to determine the forces acting on the links and joints as well as the torque applied to the crank. This study focuses on the use of mechanism design theory to synthesize each solution, which is then used to determine the configurations of the links. The use of mechanism design theory is seen as beneficial since returned solutions will satisfy a defined motion and avoid analysing solutions that are far from being acceptable. As a result, with mechanism design there is more control over the outcome of each solution. Furthermore, a dynamic analysis is performed to evaluate the joint forces and crank torques of each solution, thus taking into account inertia forces in the design. The combination of the mechanism design theory and the dynamic analysis formulates the necessary tools to perform the optimization. The optimization results will show that a large decrease in the energy of the system, as well as decreasing the maximum driving torque is obtained when compared to an initial design. A physical prototype is also constructed to demonstrate the design as a working machine and to verify the computer generated motion of the mechanism.

Acknowledgements

I would like to sincerely thank my advisor Dr. Q. C. Wu for providing me with the opportunity to pursue graduate studies. Without Dr. Wu's continuous support and guidance, as well as her encouragement during difficult periods, the completion of this thesis would not be possible. I am very grateful of the fact that if Dr. Wu never approached me to pursue graduate studies I would not have pursued it on my own.

Along with Dr. Wu, I would like to thank Dr. Subramaniam Balakrishnan and Dr. Myron Britton for their careful review, comments and suggestions with regards to this thesis. I would also like to thank all the professors who increased my knowledge in many areas, and who always gave insightful responses to any questions and concerns.

I would like to thank my fellow students who always offered their help. Even the smallest discussion would always introduce new ideas on how to overcome a problem. I would also like to thank my family and friends who have always supported me throughout my studies and who helped contribute in any way they could. More importantly, I would like to thank my father, who has spent many late nights helping me build my prototype and my loving girlfriend Ashley, who has offered continuous assistance throughout all aspects of my studies, whether it was testing throughout the night or correcting my thesis numerous times, she would do anything she could to help me.

Table of Contents

List of Figures

List of Tables

Chapter 1

1. Introduction

1.1 Introduction

It has been established that legged, off-road vehicles exhibit better mobility, obtain higher energy efficiency and provide more comfortable movement than those of conventional tracked or wheeled vehicles while moving on rough terrain [1]. In the last several decades a wide variety of leg mechanisms have been researched for the applications of legged locomotion, such as planetary exploration, walking chairs for the disabled and for military transport, rescue in radioactive zones for nuclear industries and in other hostile environments. Because these leg mechanisms require a fairly large number of links to provide high mobility, it is extremely complicated for the type selection and dimensional synthesis of leg mechanisms. Although significant progress has been made in the last few decades, there are still a number of design problems that remain unsolved, and thus requires further research.

1.2 Literature Survey

In 1770, Richard Edgeworth tried to construct a wooden horse with 8 legs to jump over high walls [2], however 40 years of experimentation was unsuccessful in constructing such a mechanism. In 1968, General Electric developed a walking truck that was capable

of walking 5 mph [3], and in 1976, Frank and McGhee made the first computer controlled walking machine [4]. More recently, a Mechatronics Research Group from the University of Southern Queensland created a pneumatically powered quadruped [5], and Applied Motion Inc, created a Spring Walker bipedal exoskeleton [6]. A more detailed list mentioning milestones in legged robots can be seen at reference [7].

Type synthesis has been one of the focuses for the early research on design of leg mechanisms, where slider-crank mechanisms [8] and multiple cam mechanisms [9] have been used. It was recommended to use only revolute joints for leg walking machines due to the difficulties in lubrication and sealing of the sliding joints, which is essential for the machines to walk outdoors [8]. Many pin-joined legged mechanisms have been designed, which are often compound mechanisms consisting of a four-bar linkage and a pantograph [8,10-13]. The potential advantages of such compound mechanisms are fast locomotion, minimal energy loss, simplicity in control design, and the slenderness of the leg as discussed in reference [14,15].

There have been many investigations on the adequate degrees-of-freedom (DOF) for each leg mechanism. Depending on the desired functional requirements (flexibility, speed, etc.) and walking environment, the legged walkers can have up to eight legs and a total of eighteen active DOF [16]. Another example is the Adaptive Suspension Vehicle, developed by Ohio State University, which has six legs and eighteen DOF [15,17]. In general, it has been accepted that three DOF for each leg is required to provide high mobility, one for providing back-and-forth, one for up-and-down motion of the foot and one for turning, [11,14,18]. However, it has been discussed that unlike a ground-based manipulator that can be operated with an off-board power supply, a walking machine has

to carry the entire power supply in addition to the external payload and the weight of the machine body. Thus, it is desirable to use a small number of actuators to reduce the body weight and to simplify the motion coordination [12]. A number of six-link and seven-link leg mechanisms have been designed with one degree-of-freedom [11-14,19]. Rigorous research has been carried out on their mobility and energy loss through kinematic and structural analysis. Two important findings have been documented: (1) a crank as an input link with continuous rotation motion should be used to achieve fast motion with minimum control [11,12,14,18], and (2) an ovoid foot path is necessary to step over small obstacles without raising the body too much [12,14,18]. These two requirements are important for designing single-DOF (SDOF) leg mechanisms for mobility and energy efficiency.

While the leg walking mechanisms have high potential in mobility and energy efficiency on rough terrain, they often involve a large number of geometrical dimensions, which makes it necessary to resort to optimization to achieve high quality design. Reducing energy loss has always been the interest in designing leg mechanisms. Other objectives include minimizing the leg height, mass, and the maximum joint torques [12,14,18]. In some research, springs were added to reduce and store the energy and to reduce the actuating torque [14]. In the process of energy optimization, force analysis of the designed mechanism is needed. Due to the complexity of the mechanisms, in previous research, the force analysis has been restricted to static analysis [12,14,19], thus neglecting the dynamics of the system. The true dynamic analysis of the mechanism has important impact on energy optimization especially when fast locomotion is to be created. Each of the optimizations seen in these papers had a common aspect of using the

link lengths of the leg as variables to control their optimization. By modifying the length of the links directly, the optimization can be compared to shooting at a target in the dark, where there is poor control on where the shot is taken and it can be very time consuming to find the bulls eye (optimal point).

While legged walking mechanisms have been designed and built based on engineering theories, they have also attracted much attention from the art fields. The kinetic sculpture "Wind Beast" is a multi-legged walking mechanism powered by wind. It was created by Mr. Theo Jansen, a Dutch kinetic sculptor. The mechanism has many advantages from the design viewpoint, such as: it has a SDOF, a crank as an input link and an ovoid foot path. Also, two legs are in pair and are mirrored, where they share the same crank as the input link. This is beneficial because a central shaft can be used to operate all the legs without adding extra actuators.

1.3 Objectives

In this work, using the leg mechanism used in Mr. Jansen's "Wind Beast", the following objectives are desired:

1) To design the leg using mechanism design theory
2) To derive the dynamics of the system
3) To optimize the leg mechanism

I will design the leg mechanism using the mechanism design theory because it gives greater control on the returned mechanisms, and can improve the efficiency of an

optimization process, which is unseen in previous research. Constraints will be applied to each solution to evaluate its validity. For evaluation purposes I derived and calculated the kinematics for each solution. The kinematic solutions are useful for two aspects of the evaluation: i) the derivation of the angles allows us to examine its motion and is necessary to evaluate the constraints, ii) the acceleration of the links is critical in the evaluation of the dynamics of the system. I then derived and evaluated the dynamics of the leg mechanism because the inertia forces of each link need to be considered, which was ignored in previous work as well. Dynamics is used to evaluate the energy consumption of the system and is used to help rank solutions during the optimization process. Finally the optimization is applied to the problem to improve the performance of the leg mechanism and to demonstrate that an optimization process can be successful with the use of mechanism design theory.

The thesis is organized as follows. Chapter 2 describes the design of Theo Jansen's mechanism as well as constraints imposed on the system. The complete design of the leg is separated into two main stages, where the second stage is dependent on the outcome of the first stage. The free choices defining the problem are also discussed. Chapter 3 describes the analysis used on the leg mechanism. There are two main categories of analysis, first is the complete kinematics of each link and second is the dynamics describing the system. Chapter 4 discusses the optimization of the leg mechanism, including the objective functions and any additional constraints imposed on the system. The objective functions focus on reducing energy and increasing the stride length. Chapter 5 discusses the results of the optimization when compared to the trial-and-error results. It goes into detail about the defining of the constraints as well as the selection of

certain constants and mass of the links. Furthermore, both results are compared and then the physical prototype is discussed. Lastly, Chapter 6 discusses the final conclusions and recommendations for future work.

Chapter 2

2. Design of a Leg Walking Mechanism

2.1 Introduction

In this chapter, the design of Theo Jansen's mechanism will be discussed. Overall, the design of the mechanism can be accomplished in two main stages. Initially when Theo Jansen designed his leg mechanism he used an optimization program that changed the lengths directly, which as a result could be very time consuming. To improve on the effectiveness of an optimization process, the use of linkage design principals were chosen to be used because each generated solution must pass through the chosen precision points. As a result, the linkage design theory will return solutions that pass through desired positions and points on a trajectory. The optimization eliminates the examination of solutions that would not fall within the area of interest; therefore, it becomes more efficient when searching because it will not be examining solutions that would never be acceptable.

Once a solution is found it must then satisfy certain constraints imposed on it to ensure that the components and behaviour of the mechanism behaves in a desired manner for the needs of the leg mechanism. Also, by examining the constraints for each solution it can determine if the mechanism is unfit before it passes on to any analysis, thus reducing computational time even further.

The chapter is organized in the following manner. First it describes Theo Jansen`s mechanism in detail by identifying each sub component of the mechanism, as well it describes the desired behaviour of the mechanism. Second it goes into detail of the design of the mechanism which is broken down into two main steps. The first step is the design of two four-bar subcomponents, and the second is the design of a parallel four-bar mechanism which is explained in greater detail later in the chapter. These include the detailed theory used to synthesize each component, as well as the number of free choices needed by the user for each solution. The last section describes the constraints imposed on the system with a description of their purpose and reasons as to why they are used.

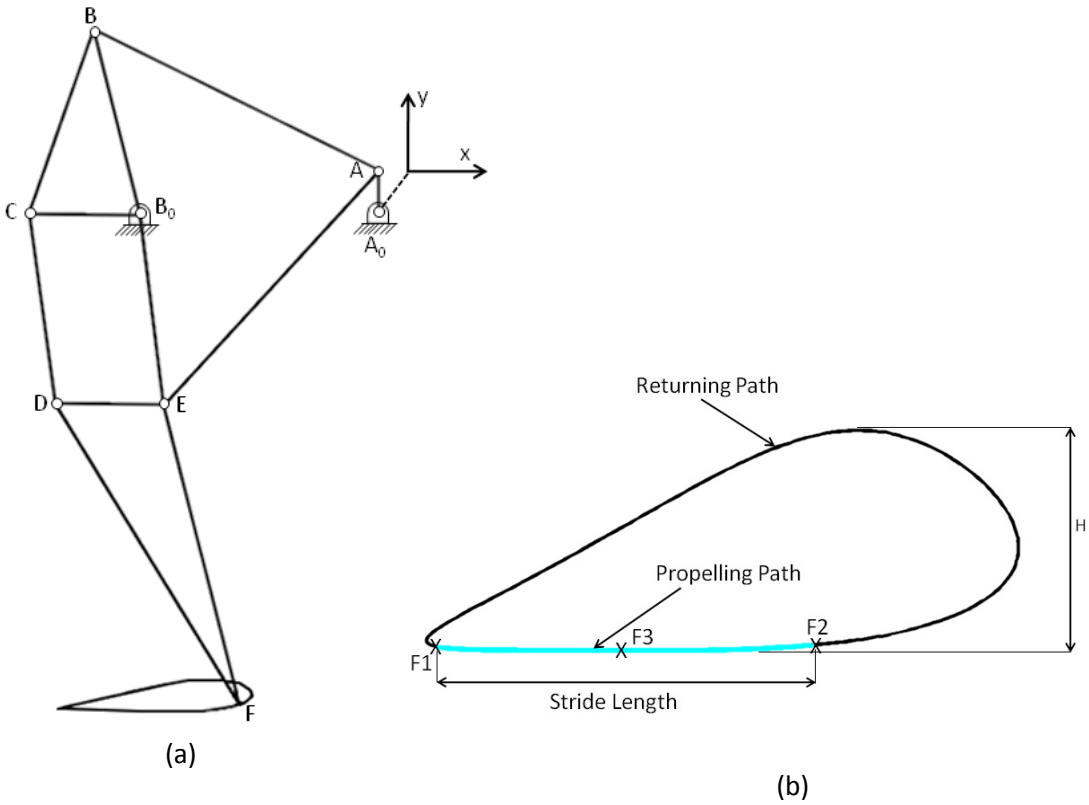

Figure 2.1: (a) Leg Mechanism and (b) Foot Profile

2.2 Mechanism Description

The planar SDOF mechanism inspired by Mr. Theo Jansen's kinetic sculpture is an eight-bar mechanism shown in Figure 2.1a, which consists of a pair of mirror-imaged four-bar mechanisms, A_0ABB_0 and A_0AEB_0, augmented with another four-bar linkage B_0CDEF, where DEF forms one rigid link. The eight-bar linkage is equivalent to a six-bar mechanism from a design viewpoint since the four-bar linkages A_0ABB_0 and A_0AEB_0 are identical in dimensions. For convenience, an X-Y coordinate system is used for this mechanism with the x and y-axes pointing to the horizontal right and upwards where its origin is located at A_0 as shown in Figure 2.1a.

To use this mechanism as a walking machine, link A_0A serves as an input link and link DEF serves as an output link with F as the tracer point, which is also called the foot-point. The leg mechanism is designed to generate an ovoid walking path for two reasons: (1) the ovoid path enables the walking mechanism to step over small obstacles without having significant elevation changes of the hip or without applying an additional DOF motion, and (2) it can also minimize the slamming effect caused by the inertia forces during walking as discussed in [11,14]. The foot-point path is composed of two portions (Figure 2.1b). First is the propelling portion, which is the flat portion of the path located between points F1 and F2. During this portion of the path, the foot-point F is in contact with the ground. The second is the returning portion, where the foot-point F is not in contact with the ground. The length of portion F1 to F2 is the stride length, and the height H is the maximum height of an obstacle that the walking machine can step over. Since the trajectory of the foot-point relative to the hip (A_0B_0) is a closed curve and A_0B_0 is

located outside the curve, a crank-rocker mechanism must be designed as discussed in [8]. Thus, in this work, A_0A is designed as a crank.

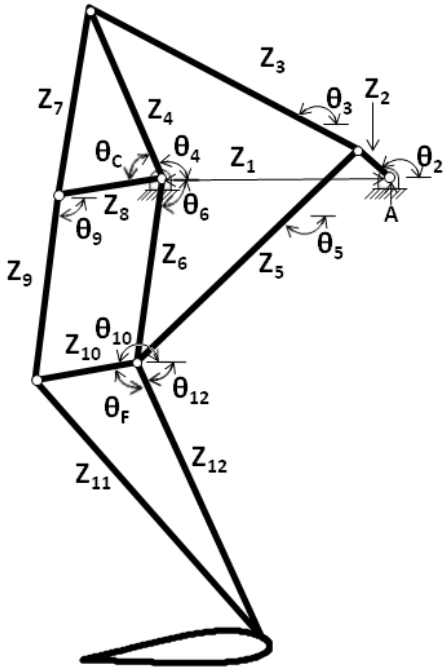

Figure 2.2: New Labelling Convention of the Links (Note: the angles are positive in the counter clockwise direction)

2.3 Mechanism synthesis

The complete synthesis of the mechanism is comprised of two steps. The first is the synthesis of the function generator (A_0ABB_0 and A_0AEB_0) using three precision points, and the second is the parallel mechanism and the foot coupler (B_0CDEF) using four precision point path generation. To simplify the notations of each link, a new convention of labelling is shown in Figure 2.2, where Z_i represents the length of the link, θ_i is the direction angle of the link Z_i, θ_c is the angle separating the links Z_4 and Z_8, and θ_F is the angle separating link Z_{10} and Z_{12}.

2.3.1 Function Generator-3 Precision Points

The first step is the synthesis of the four-bar linkages $Z_1Z_2Z_3Z_4$ and $Z_1Z_2Z_5Z_6$ (Figure 2.2), which are treated as a function generator, where Z_2 is the common input link (a crank), and Z_4 and Z_6 are the output links (rockers). The relationship between the input motion angle, and output motion angle is chosen to be described by a sinusoidal function, i.e.,

$$f(x) = y = A\sin(x - B) + C, x_0 \leq x \leq \mathrm{x_{n+1}} \tag{2.1}$$

where $x_0 \leq x \leq \mathrm{x_{n+1}}$ is the range of the function, n is the number of precision points being considered, and to be consistent with the literature [20 pg. 341-343], φ represents θ_2 in the synthesis equations and ψ represents θ_4 or θ_6. The selection of a sinusoidal function for the function generator is based on the consideration that the human hip motion can be approximated as a sinusoidal function. To design a mechanism with low vertical movement and to a certain extent, similar to the human hip motion, it was desirable to have the input and output motion to satisfy eq. (2.1) as discussed in reference [8]. Three coefficients A, B and C are used as free choices in the synthesis. Their selections will be discussed later.

2.3.1.1 Chebyshev Spacing

In the synthesis of the function generator, three precision points are used. One difficulty is the selection of the precision points because it affects the ability of the solution to replicate the desired function. An excellent initial approximation can be found with the use of Chebyshev spacing [20, pg. 341-343, 21, pg. 262-263]. By using Chebyshev

spacing, the structural error (difference between the actual and desired function) is minimized. However, if greater accuracies are needed then other methods should be used. Chebyshev spacing is defined as follows for *n* precision points,

$$x_i = \frac{1}{2}(x_{n+1} + x_0) - \frac{1}{2}(x_{n+1} + x_0)\cos\frac{(2i-1)\pi}{2n}, \quad i = 1,2,\dots,n \tag{2.2}$$

Where the precision points y_i are calculated by inserting the values of x_i back into the equation,

$$y_i = f(x_i) = A\sin(x_i - B) + C, \quad i = 1,2,\dots,n \tag{2.3}$$

After finding the precision points x_i and y_i, a desired range is given or chosen for the problem, which defines the specific range that the input (Z_2) and output (Z_4 or Z_6) link will occupy during its motion,

$$\phi_0 \le \phi \le \phi_{n+1} \quad and \quad \psi_0 \le \psi \le \psi_{n+1} \tag{2.4}$$

where φ is the angle of the input link and ψ is the angle of the output link which is used for the synthesis portion of the calculations. To calculate these precision point angles the values of φ_i has a linear relationship with x_i, and ψ_i has a linear relationship with y_i. The basic linear relationship is seen as:

$$\phi_i = ax_i + b \quad and \quad \psi_i = cy_i + d \tag{2.5}$$

Using the beginning and end point of each range, the unknown terms of a, b, c and d can be solved, thus giving the necessary equation to determine the precision points,

$$\phi_i = \frac{\phi_{n+1} - \phi_0}{x_{n+1} - x_0}(x_i - x_0) + \phi_0, \quad i = 1,2,\dots,n \tag{2.6}$$

$$\psi_i = \frac{\psi_{n+1} - \psi_0}{y_{n+1} - y_0}(y_i - y_0) + \psi_0, \quad i = 1,2,\dots,n \tag{2.7}$$

These calculated precision points can now be used with Freudenstein's method to calculate the links that satisfy the function.

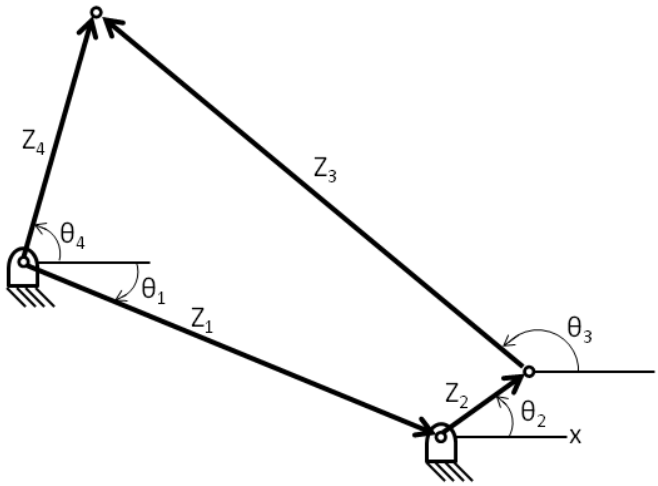

Figure 2.3: Four-Bar Mechanism Used for Function Generation

2.3.1.2 Four-Bar Function Generation

A great analytical method that is used for function generation is the techniques developed by Freudenstein. He developed a basic equation relating the input and output link of the four-bar mechanism, which is then used to synthesize the four-bar mechanism [21, pg. 260-262][22, pg. 575-577]. This method requires the angle of the input link and its corresponding angle of the output link for each precision point. Based on Figure 2.3, Freudenstein's Equation can be written in the form of φ_i and ψ_i (i=1,2,3) as:

$$K_1\cos\phi_1 + K_2\cos\psi_1 + K_3 = -\cos(\phi_1 - \psi_1) \quad (2.8)$$

$$K_1\cos\phi_2 + K_2\cos\psi_2 + K_3 = -\cos(\phi_2 - \psi_2) \quad (2.9)$$

$$K_1\cos\phi_3 + K_2\cos\psi_3 + K_3 = -\cos(\phi_3 - \psi_3) \quad (2.10)$$

where K_1, K_2 and K_3 are constants and their solution can be seen as,

$$K_1 = \frac{\omega_3\omega_5 - \omega_2\omega_6}{\omega_1\omega_5 - \omega_2\omega_4} \; and \; K_2 = \frac{\omega_1\omega_6 - \omega_3\omega_4}{\omega_1\omega_5 - \omega_2\omega_4} \tag{2.11}$$

where, (2.12)

$$\omega_1 = \cos\phi_1 - \cos\phi_2 \qquad \omega_4 = \cos\phi_1 - \cos\phi_3$$

$$\omega_2 = \cos\psi_1 - \cos\psi_2 \qquad \omega_5 = \cos\psi_1 - \cos\psi_3$$

$$\omega_3 = -\cos(\phi_1 - \psi_1) + \cos(\phi_2 - \psi_2) \qquad \omega_6 = -\cos(\phi_1 - \psi_1) + \cos(\phi_3 - \psi_3)$$

$$K_3 = -\cos(\phi_i - \psi_i) - K_1\cos\phi_i - K_2\cos\psi_i \;,\; i = 1, 2, or\; 3 \tag{2.13}$$

To calculate the solution, the user is required to make one free choice consisting of the length of link Z_1. With this choice the remaining lengths (Z_2, Z_3 and Z_4) can be calculated using the following:

$$Z_4 = \frac{Z_1}{K_1} \tag{2.14}$$

$$Z_2 = -\frac{Z_1}{K_2}$$

$$Z_3 = \sqrt{2K_3Z_2Z_4 + Z_1^2 + Z_2^2 + Z_4^2}$$

With the free choice of the ground spacing Z_1, the lengths of Z_2, Z_3 and Z_4 are returned. During the synthesis of the function generator, the relationship between the input and output motion defined by eq. (2.1) is not prescribed. They are determined using either trial-and-error or with the use of the optimization procedure discussed later.

With function generation there are developed methods that utilize four or more precision points. However, when I experimented with four precision points it was found that the method was far less efficient for the needs of the desired mechanism. The efficiency of

the method was in regards to the type of mechanism that was returned. For Theo Jansen's leg mechanism it is required that the two four-bar mechanisms are of the crank-rocker variety. When compared to Freudenstein's method using three precision points, it was found that using four precision points [23] required more effort to achieve this crank-rocker mechanism.

2.3.1.3 Coupler Design, $Z_4Z_7Z_8$

Freudenstein's method does not determine the size of the coupler $Z_4Z_7Z_8$ (Figure 2.2) except for the length of Z_4. Therefore, the user has two more free choices to define the size of the coupler. One is the angle separating Z_4 and Z_8 (θ_c) and the second is the length of Z_8 (Figure 2.2). However, the choice of the angle θ_c has restrictions with its choice. If the chosen angle is too large or too small the parallelogram will reach a dead center, where the component $Z_6Z_8Z_9Z_{10}$ will jam. Based on the solution of the four-bar mechanisms, an approximate range of acceptable values can be calculated for the coupler angle. This is done by examining the angle $\measuredangle BB_0E$ (where the angle is calculated going counter clockwise from link Z_4 to Z_6) over a full crank rotation because, based on the assumption that the mechanism $Z_6Z_8Z_9Z_{10}$ is a perfect parallelogram, in theory the mechanism will always function if $0° \leq \angle BB_0E \leq 180°$. By satisfying this range, the following range for θ_c can be found using the following criteria:

$$\theta_{cmax} = \angle BB_0E_{min} \tag{2.15}$$

$$if\ \angle BB_0E_{max} > 180° \quad then \quad \theta_{cmin} = \angle BB_0E_{max} - 180° \qquad if\ \angle BB_0E_{max} < 180° \quad then \quad \theta_{cmin} = 0° \tag{2.16}$$

where $\angle BB_0E_{min}$ and $\angle BB_0E_{max}$ are the minimum and maximum calculated angles over an entire crank rotation. θ_{cmin} and θ_{cmax} are the lower and higher end of the range of possible values which can be chosen for the free choice θ_c. In the situation that $\theta_{cmin} > \theta_{cmax}$, then no matter what choice a user makes the mechanism will not function.

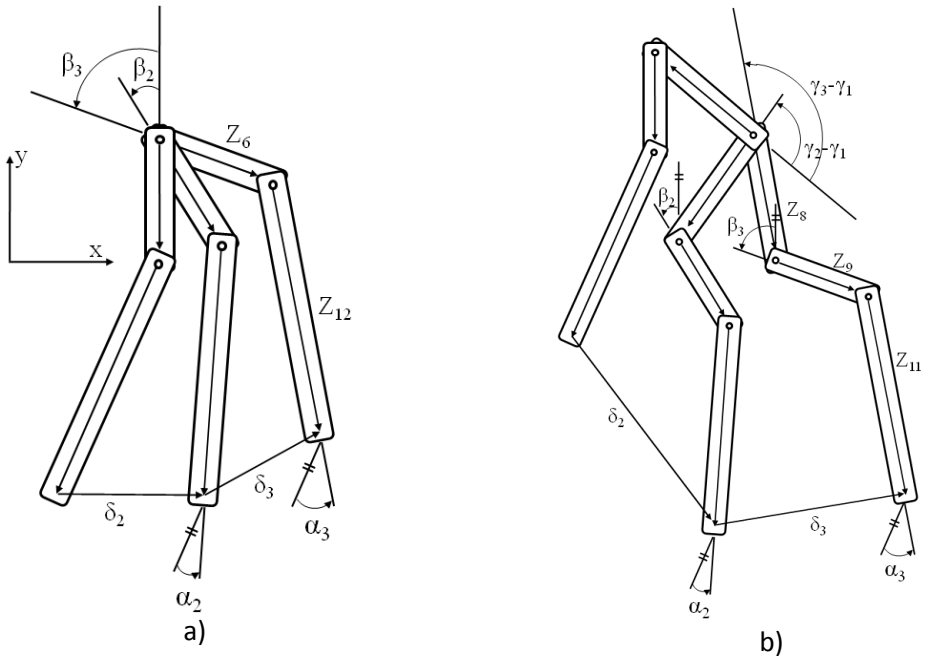

Figure 2.4: Three Out of Four Positions of the a) Standard Dyad and b) Triad

2.3.2 Path Generator-Four Precision Points

The second step is the design of mechanism $Z_6Z_8Z_9Z_{11}Z_{12}$ (Figure 2.2) as a path generator using four precision points, where the dyad Z_6Z_{12} and the triad $Z_8Z_9Z_{11}$ are synthesized separately (Figure 2.4). The solution is obtained by solving the complex equations describing the change between position 1 and i (i=2,3,4) [24, pg 180-183]:

$$\begin{bmatrix} e^{i\beta_2}-1 & e^{i\alpha_2}-1 \\ e^{i\beta_3}-1 & e^{i\alpha_3}-1 \\ e^{i\beta_4}-1 & e^{i\alpha_4}-1 \end{bmatrix} \begin{bmatrix} Z_6 \\ Z_{12} \end{bmatrix} = \begin{bmatrix} \delta_2 \\ \delta_3 \\ \delta_4 \end{bmatrix} \tag{2.17}$$

where β_i (i=2,3,4) is the change in rotation of the link Z_6, α_i represents the change in rotation of the link Z_{12}, and δ_i is the displacement vector between the first and the i^{th} precision points shown in Figure 2.4a. Similar equations can be derived for the triad, $Z_8Z_9Z_{11}$, with four precision points.

The synthesis of the triad $Z_8Z_9Z_{11}$ (Figure 2.4b) is performed using a slight modification to eq. (2.17) because an additional rotating link Z_8 is a part of the synthesis problem, however the length and position of Z_8 is known. The base equations used for the triad is seen below:

$$\begin{bmatrix} e^{i\beta_2}-1 & e^{i\alpha_2}-1 & e^{i\gamma_2}-e^{i\gamma_1} \\ e^{i\beta_3}-1 & e^{i\alpha_3}-1 & e^{i\gamma_3}-e^{i\gamma_1} \\ e^{i\beta_4}-1 & e^{i\alpha_4}-1 & e^{i\gamma_4}-e^{i\gamma_1} \end{bmatrix} \begin{bmatrix} Z_9 \\ Z_{11} \\ Z_8 \end{bmatrix} = \begin{bmatrix} \delta_2 \\ \delta_3 \\ \delta_4 \end{bmatrix} \tag{2.18}$$

where γ is the angle of link Z_8, β_i is the change in rotation of the link Z_9, and α_i is the change in rotation of link Z_{11}. Moving the known elements of eq. (2.18) over to the right side I get:

$$\begin{bmatrix} e^{i\beta_2}-1 & e^{i\alpha_2}-1 \\ e^{i\beta_3}-1 & e^{i\alpha_3}-1 \\ e^{i\beta_4}-1 & e^{i\alpha_4}-1 \end{bmatrix} \begin{bmatrix} Z_9 \\ Z_{11} \end{bmatrix} = \begin{bmatrix} \delta_2 - Z_8(e^{i\gamma_2}-e^{i\gamma_1}) \\ \delta_3 - Z_8(e^{i\gamma_3}-e^{i\gamma_1}) \\ \delta_4 - Z_8(e^{i\gamma_4}-e^{i\gamma_1}) \end{bmatrix} = \begin{bmatrix} \delta_2^* \\ \delta_3^* \\ \delta_4^* \end{bmatrix} \tag{2.19}$$

where δ_i^* represents the modified right side of the equation and eq. (2.19) is in the suitable form where the synthesis procedure can be applied. For this method it is required that α_i and δ_i (i=2,3,4) are predefined with the free choice of β_2. The free choice β_2 is chosen separately for the synthesis of the dyad and triad, where α_i and δ_i are the same

values for both. With this information the following equations are used to solve for the unknown angles β_3 and β_4:

$$\Delta_2 = \begin{vmatrix} e^{i\alpha_3} - 1 & \delta_3 \\ e^{i\alpha_4} - 1 & \delta_4 \end{vmatrix}$$

$$\Delta_3 = -\begin{vmatrix} e^{i\alpha_2} - 1 & \delta_2 \\ e^{i\alpha_4} - 1 & \delta_4 \end{vmatrix} \tag{2.20}$$

$$\Delta_4 = \begin{vmatrix} e^{i\alpha_2} - 1 & \delta_2 \\ e^{i\alpha_3} - 1 & \delta_3 \end{vmatrix}$$

$$\Delta_1 = -\Delta_2 - \Delta_3 - \Delta_4 \tag{2.21}$$

$$\Delta = \Delta_1 + \Delta_2 e^{i\beta_2} \tag{2.22}$$

$$\cos\theta_3 = \frac{|\Delta_4|^2 - |\Delta_3|^2 - |\Delta|^2}{|2\Delta_3\Delta|} \tag{2.23}$$

$$\sin\theta_3 = |(1 - \cos^2\theta_3)^{1/2}| \geq 0 \tag{2.24}$$

$$\theta_3 = \tan^{-1}\frac{\sin\theta_3}{\cos\theta_3} \tag{2.25}$$

$$\beta_3 = \arg\Delta + \theta_3 - \arg\Delta_3 \tag{2.26}$$

$$\cos\theta_4 = \frac{|\Delta_3|^2 - |\Delta_4|^2 - |\Delta|^2}{|2\Delta_4\Delta|} \tag{2.27}$$

$$\sin\theta_4 = |(1 - \cos^2\theta_4)^{1/2}| \geq 0 \tag{2.28}$$

$$\theta_4 = \tan^{-1}\frac{\sin\theta_4}{\cos\theta_4} \tag{2.29}$$

$$\beta_4 = \arg\Delta + \theta_4 - \arg\Delta_4 \tag{2.30}$$

The angles β_3 and β_4 are solved in a way that the three linear equations found within eq. (2.17) or eq. (2.19) will behave like 2 linear equations. Therefore, all of the unknowns in eq. (2.17) or eq. (2.19) are known except for Z_6 and Z_{12} or Z_9 and Z_{11}. These unknowns

can be solved directly by solving two of the three equations within eq. (2.17) or eq. (2.19), where the solution will also satisfy the third linear equation.

One difficulty with the synthesis is that the desired or optimal path or motion is not defined or known. Therefore, the four precision points (P_1, P_2, P_3 and P_4) have to be chosen as well as the rotations (α_2, α_3 and α_4) of link Z_{12} and Z_{11}, where α_i is the rotation from position 1 to position i of link $Z_{10}Z_{11}Z_{12}$ (Figure 2.2).

Another difficulty with the second stage of the synthesis is that it is dependent on stage one. Hence, the lengths and directions of Z_6 and Z_8 are already determined. Therefore, for each precision point, the direction of link Z_6 and Z_8 needs to be known because with the synthesis of the dyad, the returned length and direction of Z_6 must be the same as precision point one to satisfy the first stage of the design. With the triad, the length and direction of Z_8 must be known so that the loop closure equation describing the triad can be put in the form needed for the synthesis method. To choose the direction of the links Z_6 and Z_8 the direction of the crank (Z_2) can be defined for each of the four precision points (θ_{2a}, θ_{2b}, θ_{2c}, θ_{2d} are the chosen crank angles at precision points P_1, P_2, P_3 and P_4). Since the mechanism has a SDOF, the angles of every link can be determined when the direction of the crank (Z_2) is defined.

To define the precision points I defined the length and angle of Z_{12} at each of the four desired crank directions for each precision point. Since the direction of Z_6 is known, the location of the precision point is the addition of the link Z_6 and Z_{12}. The value for α_i is the difference in the chosen angles for the link Z_{12} between precision point 1 and i.

2.3.3 Free Choices

Together with the design of the function generator, there are a total of nineteen free choices which are the three parameters A, B, and C as shown in eq. (2.1), the desired ranges of the input and output links, $\phi_0 \leq \phi \leq \phi_{n+1}\ and\ \psi_0 \leq \psi \leq \psi_{n+1}$, the ground link Z_1 of the function generator, the coupler angle θ_c, the length Z_8, the four angles defining the direction of Z_{12} at each precision point, the length of Z_{12} and the four crank angles corresponding to each precision point. Once these free choices are selected, the dimensions of the legged mechanism (Figure 2.2) can be determined using the previously mentioned methods. In this work, such free choices will be selected using two separate methods: trial-and-error and optimization as discussed later. A set of constraints must be satisfied in order to exhibit acceptable motion, which is discussed in the following section.

2.4 Constraints

Each time a solution is found it must satisfy a set of constraints to be considered an acceptable solution. Mechanism constraints are criteria that are imposed on the geometry of the linkage, stride length, mechanism type, etc.

Constraint #1 - Grashof Criteria

The two four-bar mechanisms used in the leg mechanism must be crank-and-rocker mechanisms to be successful. This is verified by checking the Grashof criterion [25, pg.

27-28] where two properties need to be satisfied. The first is that the crank must be the shortest link:

$$C1 \coloneqq Z_2 \leq \min\left[Z_1, Z_3, Z_4\right] \tag{2.31}$$

Constraint #2 - Grashof Criteria

The second property is the sum of the shortest and longest link must be smaller than the sum of the remaining two links:

$$C2 \coloneqq x_1 + x_2 < x_3 + x_4 \tag{2.32}$$

where x_1 and x_2 are the shortest and longest links, x_3 and x_4 are the remaining two links.

Constraint #3 - Stride Length

The stride length, as previously mentioned, is the distance between the points F1 and F2 (Figure 2.1b). To avoid unsatisfactory designs, the stride length must be above a specified amount (HC1), if not the design is rejected:

$$C3 \coloneqq \left|F_1 - F_2\right| \geq HC1 \tag{2.33}$$

Constraint #4 - $Z_6Z_8Z_9Z_{10}$ Inner Angles

Some designs for the $Z_6Z_8Z_9Z_{10}$ mechanism component (Figure 2.2) of the leg can return solutions where the mechanism will jam when the mechanism exceeds its range of motion. Therefore, the angle in the four inner corners of the $Z_6Z_8Z_9Z_{10}$ mechanism is checked throughout the cycle. If it goes below or above a set range the mechanism is rejected:

$$C4 \coloneqq HC2 \leq \theta_P, \theta_Q, \theta_R, \theta_S \leq HC3 \tag{2.34}$$

where θ_p is the angle separating link Z_6 and Z_8, θ_Q separates link Z_8 and Z_9, θ_R separates link Z_9 and Z_{10}, and θ_S separates link Z_6 and Z_{10}.

Constraint #5 - Stride Path Behaviour

The foot path needs to be checked to ensure that two events occur: a) the foot path along the ground needs to be flat and b) the foot does not come into contact with the ground during its return path. To check if the foot path is along the ground, the program finds the lowest vertical point (F3 - Figure 2.1b) along the foot path. Any point that is within a very small vertical range (HC4) of the point is considered along the ground because some deviation is expected while it is walking. Therefore, the program checks if any points between the calculated extremities lift off the ground, if so then the solution is rejected. The crank angles corresponding to the two extremities of the path along the ground are α_1 and α_2, where α_1 is when the foot makes contact with the ground and α_2 is when the foot leaves the ground:

$$C5 := Y_F|_{\alpha=\alpha_1\rightarrow\alpha_2} \leq Y_{Fmin} + HC4 \tag{2.35}$$

where Y_F represents the y coordinates of the foot path.

Constraint #6 - Return path behaviour

Similar to constraint #5, the return path needs to be checked to see if any points are considered to be in contact with the ground during the return path. If so then the solution is rejected:

$$C6 := Y_F|_{\alpha=\alpha_2\rightarrow\alpha_1} \geq Y_{Fmin} + HC4 \tag{2.36}$$

Constraint #7 – Component behaviour Z_6Z_{12}

It is desired that the leg mechanism design will have the parallel mechanism component ($Z_6Z_8Z_9Z_{10}$, Figure 2.2) in each design. However, this cannot be achieved for all solutions because it is based on the solution returned from the synthesis. As previously mentioned, the synthesis of the parallel mechanism and the foot coupler requires one free choice for each dyad and triad and the user specification of the angles α_i. Prior to the synthesis, the direction and length of Z_6 and the location of the precision points are known. An exhaustive search is performed in Matlab on the free choice β_2 to calculate a solution that matches the same length and direction of Z_6 in its first precision point orientation, where β_2 is the rotation of link Z_6 from precision point one to two. The exhaustive search weighs the solutions based on the difference between the real and desired values:

$$min\{C7 := |Z_{6desired} - Z_{6actual}| + |\theta_{6desired} - \theta_{6actual}| + |Prec1_{desired} - Prec1_{actual}|\} \quad (2.37)$$

where Prec1 are the coordinates of the first precision point.

Constraint #8 - Component behaviour $Z_8Z_9Z_{11}$

Very similar to constraint #7, the same occurs for the dyad Z_9 and Z_{11}, where Z_9 should be the same length and angle as Z_6 but it is not as critical. β_2 is now the rotation of link Z_9 from precision point one to two. The exhaustive search weighs the solutions based on the difference between the real and desired values:

$$min\{C8 := |Z_{6desired} - Z_{9actual}| + |\theta_{6desired} - \theta_{9actual}| + |Prec1_{desired} - Prec1_{actual}|\} \quad (2.38)$$

2.5 Summary

This chapter describes the theory and techniques needed to design the leg mechanism using engineering principals. The benefits of using this theory is that it is more efficient at returning acceptable solutions that behave in a desirable manner when compared to strictly changing the lengths of the links as used in previous work. This avoids the tedious analysis of unsuitable mechanisms that would never be considered. The linkage design theory requires a larger amount of variables for the problem than that of just changing the link lengths directly. However, the higher efficiency of returning more suitable solutions outweighs the larger number of variables needed to design the leg.

The constraints of the system are very important in the design and optimization of the mechanism. Previous works with optimizations all included constraints to help force a solution to satisfy specific requirements and can be used to identify if a solution is acceptable for the design goals. By identifying if a solution is unacceptable, the analysis portion of the optimization can be ignored, thus saving computational time.

Furthermore, the linkage design theory allows the user to have a greater influence on the solution output. These can be certain specifics associated with the path behaviour of the foot. The choice of the precision points allows the user to specify certain behaviours such as a higher height of the foot path, or separating the precision points to achieve a longer step length. However, some experience is needed, because after examining the effect of changing the precision points, one can notice that certain sets of precision points will

return more or better solutions than others. Like many design problems, some knowledge and experience on the choice of these precision points aids with their selection.

Chapter 3

3. Analysis

3.1 Introduction

After a solution is obtained using the mechanism design theory, the question of "is the solution valid and how well does it perform?" is always asked. Chapter 2 discussed the application of constraints on the system to check if it was valid. However, to examine some of the constraints additional analysis is required. In terms of the constraints, it needs a positional analysis to examine the motion of all the links as well as the tracer path of the foot. Motion analysis is also required to estimate the acceptable range of the coupler angle (θ_c, Figure 2.2) that can be made as a free choice by the user.

Looking further into the analysis, it is desirable to evaluate the mechanism in a way that examines the energy consumption of the leg mechanism. In previous work, the research only examines static forces, thus neglecting dynamic effects. As a result, to examine the dynamics of these systems it is first necessary to calculate the kinematic information (direction, velocity and acceleration) of each link for the given kinematics of the crank over an entire cycle of the system. Second, with the use of this information, the dynamics of the system can be calculated. However, the dynamic equations describing the mechanism need to be derived for each individual link. The equations can then be added together to form a full matrix representing the total system. One problem that arises is

that there are too many unknowns for equations. More specifically, there are two unknowns that need to be defined. These are the x and y-component reaction forces between the foot and the ground, however these unknowns become zero when the foot is in the air. The equations can be solved with an assumption about the reaction forces acting between the ground and the foot which is a similar problem in previous research [11,12,14,19].

The organization of this chapter is as follows; first the chapter will describe the kinematic equations used to determine all the unknown angles, velocity and acceleration for each link. Second there is a discussion on the dynamics of the system, where it mentions the assumptions applied to the mechanism as well as the generic dynamic equations for both the binary and tertiary link situation. Then the complete derivation for each link is given.

3.2 Kinematic Analysis

The kinematic analysis is very important to understand the motion of the mechanism and is needed to perform the dynamic analysis discussed in Section 3.3. The positional analysis is performed by separating the mechanism into three separate loops ($Z_1Z_2Z_3Z_4$, $Z_1Z_2Z_5Z_6$ and $Z_6Z_8Z_9Z_{10}$, Figure 3.1-3.3). Writing the loop closure equation for each loop [26, pg. 120-125], the complete kinematic information can be determined for each link. However, the complete kinematics of a single link needs to be known to perform the analysis. In this case the crank is defined as having a constant angular velocity. Since the kinematics of the crank are defined, the kinematics of loop 1 ($Z_1Z_2Z_3Z_4$) and loop 2

($Z_1Z_2Z_5Z_6$) need to be solved first before solving loop 3 ($Z_6Z_8Z_9Z_{10}$). The complete derivations are described in the following sections.

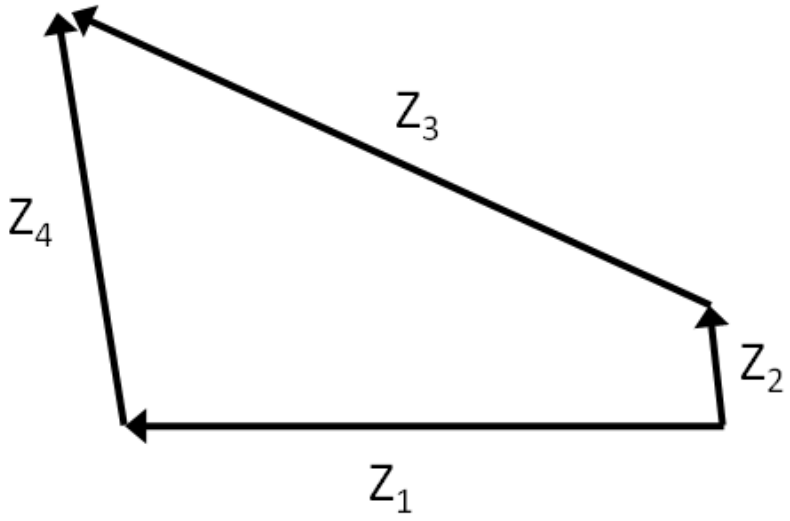

Figure 3.1: Loop Closure Diagram, Loop 1 ($Z_1Z_2Z_3Z_4$)

3.2.1 Kinematics Loop 1 – $Z_1Z_2Z_3Z_4$

Based on the kinematic information of the crank, the kinematics is solved using the following equations which are separated into three separate sub-analyses: angular direction, angular velocity and angular acceleration.

Angular Direction Analysis:

Using the equation describing the position of the upper four-bar $Z_1Z_2Z_3Z_4$ (Figure 3.1):

$$Z_1 e^{i\theta_1} + Z_4 e^{i\theta_4} = Z_2 e^{i\theta_2} + Z_3 e^{i\theta_3} \tag{3.1}$$

where θ_i is the direction angle of link Z_i. I can compute the unknown angles of θ_3 and θ_4. First, separating eq. (3.1) into its real and imaginary components:

$$Z_1\cos\theta_1 + Z_4\cos\theta_4 = Z_2\cos\theta_2 + Z_3\cos\theta_3 \quad (3.2)$$

$$Z_1\cos\theta_1 + Z_4\sin\theta_4 = Z_2\sin\theta_2 + Z_3\sin\theta_3 \quad (3.3)$$

Rearranging eq. (3.2) and eq. (3.3) I get:

$$Z_4\cos\theta_4 = C + Z_3\cos\theta_3 \quad (3.4)$$

$$Z_4\sin\theta_4 = D + Z_3\sin\theta_3 \quad (3.5)$$

where,

$$C = Z_2\cos\theta_2 - Z_1\cos\theta_1$$

$$D = Z_2\sin\theta_2 - Z_1\sin\theta_1$$

If I square and add eqns. (3.4) and (3.5) I will then get:

$$Z_4^2 = C^2 + 2Z_3C\cos\theta_3 + Z_3^2 + D^2 + 2DZ_3\sin\theta_3 \quad (3.6)$$

Rearranging eq. (3.6) and grouping the known values together will give:

$$2Z_3C\cos\theta_3 = E + 2DZ_3\sin\theta_3 \quad (3.7)$$

where,

$$E = C^2 + Z_3^2 - Z_4^2 + D^2$$

If I replace $\cos\theta_3 = \sqrt{1 - \sin^2\theta_3}$ in eq. (3.7) and squaring the equation will give:

$$4Z_3^2C^2(1 - \sin^2\theta_3) = E^2 + 4DEZ_3\sin\theta_3 + 4D^2Z_3^2\sin^2\theta_3 \quad (3.8)$$

Rearranging eq. (3.8) gives:

$$0 = \text{asin}^2\,\theta_3 + b\sin\theta_3 + c \tag{3.9}$$

where,

$$a = 4Z_3^2(Z_2^2 - 2Z_1Z_2\cos(\theta_1 - \theta_2) + Z_1^2)$$

$$b = 4\,Z_3(Z_2\sin\theta_2 - Z_1\sin\theta_1)(Z_2^2 - 2Z_1Z_2\cos(\theta_1 - \theta_2) + Z_1^2 + Z_3^2 - Z_4^2)$$

$$c = (Z_2^2 - 2Z_1Z_2\cos(\theta_1 - \theta_2) + Z_1^2 + Z_3^2 - Z_4^2)^2 - 4Z_3^2(Z_2^2\cos^2\theta_2 - 2Z_1Z_2\cos\theta_1\cos\theta_2 + Z_1^2\cos^2\theta_1)$$

Using the quadratic formula to solve for θ_3 in eq. (3.9):

$$\theta_3 = \sin^{-1}\left[\frac{-b \pm \sqrt{b^2 - 4ac}}{2a}\right] \tag{3.10}$$

Assuming that θ_3 is calculated I can then solve for θ_4 by rearranging eq. (3.4) that will return:

$$\theta_4 = \cos^{-1}\left[\frac{Z_2\cos\theta_2 - Z_1\cos\theta_1 + Z_3\cos\theta_3}{Z_4}\right] \tag{3.11}$$

Therefore all the angles would be known within loop 1.

Angular Velocity Analysis:

Taking the time derivative of eq. (3.1) gives the equation describing the velocity of Loop 1:

$$\dot{\theta}_4 iZ_4 e^{i\theta_4} = \dot{\theta}_2 iZ_2 e^{i\theta_2} + \dot{\theta}_3 iZ_3 e^{i\theta_3} \tag{3.12}$$

Separating eq. (3.12) into its imaginary components:

$$\dot{\theta}_4 Z_4 \cos\theta_4 = \dot{\theta}_2 Z_2 \cos\theta_2 + \dot{\theta}_3 Z_3 \cos\theta_3 \tag{3.13}$$

Rearranging, I get the equation describing the velocity $\dot{\theta}_4$ as a function of the unknown $\dot{\theta}_3$:

$$\dot{\theta}_4 = \frac{\dot{\theta}_2 Z_2 \sin\theta_2 + \dot{\theta}_3 Z_3 \sin\theta_3}{Z_4 \sin\theta_4} \tag{3.14}$$

Separating eq. (3.12) into its real components:

$$\dot{\theta}_4 Z_4 \sin\theta_4 = \dot{\theta}_2 Z_2 \sin\theta_2 + \dot{\theta}_3 Z_3 \sin\theta_3 \tag{3.15}$$

Inserting eq. (3.14) into eq. (3.15):

$$\dot{\theta}_2 Z_2 \sin\theta_2 + \dot{\theta}_3 Z_3 \sin\theta_3 = \tan\theta_4 (\dot{\theta}_2 Z_2 \cos\theta_2 + \dot{\theta}_3 Z_3 \cos\theta_3) \tag{3.16}$$

Rearranging eq. (3.16) to isolate for $\dot{\theta}_3$:

$$\dot{\theta}_3 = \frac{\dot{\theta}_2 Z_2 (\sin\theta_2 - \tan\theta_4 \cos\theta_2)}{Z_3 (\cos\theta_3 \tan\theta_4 - \sin\theta_3)} \tag{3.17}$$

Solving for the velocity $\dot{\theta}_3$ will allow the calculation of eq. (3.14) to find $\dot{\theta}_4$. Therefore, all the velocities in loop 1 can be solved.

Angular Acceleration Analysis:

Taking the time derivative of eq. (3.12) gives the equation describing the acceleration of loop 1:

$$Z_4\left(-\dot{\theta}_4^2 + \ddot{\theta}_4 i\right)e^{i\theta_4} = Z_2\left(-\dot{\theta}_2^2 + \ddot{\theta}_2 i\right)e^{i\theta_2} + Z_3\left(-\dot{\theta}_3^2 + \ddot{\theta}_3 i\right)e^{i\theta_3} \quad (3.18)$$

Separating the real components from eq. (3.18):

$$Z_4\left(\dot{\theta}_4^2\cos\theta_4 + \ddot{\theta}_4\sin\theta_4\right) = Z_2\left(\dot{\theta}_2^2\cos\theta_2 + \ddot{\theta}_2\sin\theta_2\right) + Z_3\left(\dot{\theta}_3^2\cos\theta_3 + \ddot{\theta}_3\sin\theta_3\right) \quad (3.19)$$

Rearranging to isolate for $\ddot{\theta}_4$:

$$\ddot{\theta}_4 = \frac{A + Z_3\ddot{\theta}_3\sin\theta_3}{Z_4\sin\theta_4} \quad (3.20)$$

where A represents the known variables in the equation:

$$A = Z_2\left(\dot{\theta}_2^2\cos\theta_2 + \ddot{\theta}_2\sin\theta_2\right) + Z_3\dot{\theta}_3^2\cos\theta_3 - Z_4\dot{\theta}_4^2\cos\theta_4 \quad (3.21)$$

Separating the imaginary components from eq. 3.18:

$$Z_4\left(-\dot{\theta}_4^2\sin\theta_4 + \ddot{\theta}_4\cos\theta_4\right) = Z_2\left(-\dot{\theta}_2^2\sin\theta_2 + \ddot{\theta}_2\cos\theta_2\right) + Z_3\left(-\dot{\theta}_3^2\sin\theta_3 + \ddot{\theta}_3\cos\theta_3\right) \quad (3.22)$$

Rearranging to isolate for $\ddot{\theta}_4$:

$$\ddot{\theta}_4 = \frac{B + Z_3\ddot{\theta}_3\cos\theta_3}{Z_4\cos\theta_4} \quad (3.23)$$

where B represents the known variables in the equation:

$$B = Z_2\left(-\dot{\theta}_2^2\sin\theta_2 + \ddot{\theta}_2\cos\theta_2\right) - Z_3\dot{\theta}_3^2\sin\theta_3 + Z_4\dot{\theta}_4^2\sin\theta_4 \quad (3.24)$$

Setting eq. (3.20) equal to eq. (3.23):

$$\frac{A + Z_3\ddot{\theta}_3\sin\theta_3}{Z_4\sin\theta_4} = \frac{B + Z_3\ddot{\theta}_3\cos\theta_3}{Z_4\cos\theta_4} \tag{3.25}$$

Rearranging to isolate for $\ddot{\theta}_3$:

$$\ddot{\theta}_3 = \frac{B\tan\theta_4 - A}{Z_3(\sin\theta_3 - \cos\theta_3\tan\theta_4)} \tag{3.26}$$

With the calculation of eq. (3.26), the eq. (3.23) or eq. (3.20) can be used to calculate $\ddot{\theta}_4$ to solve all the accelerations in loop 1.

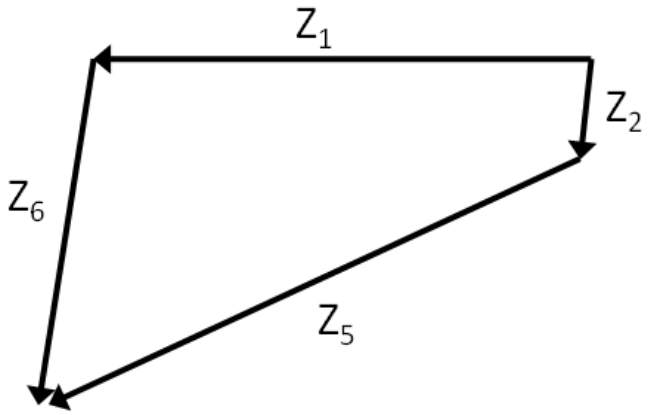

Figure 3.2: Loop Closure Diagram, Loop 2 ($Z_1Z_2Z_5Z_6$)

3.2.2 Kinematics Loop 2 – $Z_1Z_2Z_5Z_6$

The derivations of the kinematics are derived in the same manner as loop 1, except the terms for links Z_4 and Z_3 are replaced with Z_6 and Z_5 (Figure 3.2). The basic loop closure equation describing loop 2 is:

$$Z_1e^{i\theta_1} + Z_6e^{i\theta_6} = Z_2e^{i\theta_2} + Z_5e^{i\theta_5} \tag{3.27}$$

Based on eq. (3.27) and the methods used in Section 3.2.1, the following equations describing the kinematics are derived:

Angular Direction Analysis:

$$a = 4Z_5^2(Z_2^2 - 2Z_1Z_2\cos(\theta_1 - \theta_2) + Z_1^2)$$

$$b = 4\,Z_5(Z_2\sin\theta_2 - Z_1\sin\theta_1)(Z_2^2 - 2Z_1Z_2\cos(\theta_1 - \theta_2) + Z_1^2 + Z_5^2 - Z_6^2)$$

$$c = (Z_2^2 - 2Z_1Z_2\cos(\theta_1 - \theta_2) + Z_1^2 + Z_5^2 - Z_6^2)^2 - 4Z_5^2(Z_2^2\cos^2\theta_2 - 2Z_1Z_2\cos\theta_1\cos\theta_2 + Z_1^2\cos^2\theta_1)$$

$$\theta_5 = \sin^{-1}\left[\frac{-b \pm \sqrt{b^2 - 4ac}}{2a}\right] \tag{3.28}$$

$$\theta_6 = \cos^{-1}\left[\frac{Z_2\cos\theta_2 - Z_1\cos\theta_1 + Z_5\cos\theta_5}{Z_6}\right] \tag{3.29}$$

Angular Velocity Analysis:

$$\dot{\theta}_6 = \frac{\dot{\theta}_2 Z_2\sin\theta_2 + \dot{\theta}_5 Z_5\sin\theta_5}{Z_6\sin\theta_6} \tag{3.30}$$

$$\dot{\theta}_5 = \frac{\dot{\theta}_2 Z_2(\sin\theta_2 - \tan\theta_6\cos\theta_2)}{Z_5(\cos\theta_5\tan\theta_6 - \sin\theta_5)} \tag{3.31}$$

Angular Acceleration Analysis:

$$A = Z_2\left(\dot{\theta}_2^2\cos\theta_2 + \ddot{\theta}_2\sin\theta_2\right) + Z_5\dot{\theta}_5^2\cos\theta_5 - Z_6\dot{\theta}_6^2\cos\theta_6 \tag{3.32}$$

$$B = Z_2\left(-\dot{\theta}_2^2\sin\theta_2 + \ddot{\theta}_2\cos\theta_2\right) - Z_5\dot{\theta}_5^2\sin\theta_5 + Z_6\dot{\theta}_6^2\sin\theta_6 \tag{3.33}$$

$$\ddot{\theta}_5 = \frac{B\tan\theta_6 - A}{Z_5(\sin\theta_5 - \cos\theta_5\tan\theta_6)} \tag{3.34}$$

$$\ddot{\theta}_6 = \frac{B + Z_5\ddot{\theta}_5\cos\theta_5}{Z_6\cos\theta_6} \tag{3.35}$$

where A and B represents the known variables in the equation.

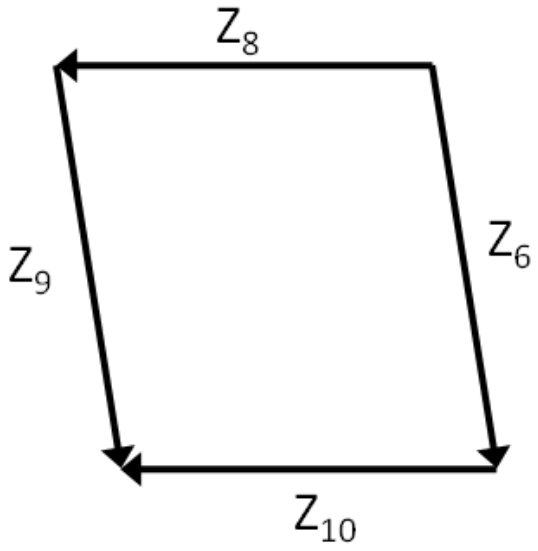

Figure 3.3: Loop Closure Diagram, Loop 3 ($Z_6Z_8Z_9Z_{10}$)

3.2.3 Kinematics Loop 3 – $Z_6Z_8Z_9Z_{10}$

The derivations of the kinematics are derived in the same manner as loop 1, except the terms for links Z_1, Z_2, Z_3 and Z_4 are replaced with Z_8, Z_6, Z_{10} and Z_9. The basic loop closure equation describing loop 3 (Figure 3.3) is:

$$Z_{10}e^{i\theta_{10}} + Z_6e^{i\theta_6} = Z_8e^{i\theta_8} + Z_9e^{i\theta_9} \tag{3.36}$$

Based on eq. (3.36) and the methods used in Section 3.2.1, the following equations describing the kinematics are derived:

Angular Direction Analysis:

$$Z_8 e^{i\theta_8} + Z_9 e^{i\theta_9} = Z_6 e^{i\theta_6} + Z_{10} e^{i\theta_{10}} \tag{3.37}$$

$$a = 4Z_{10}^2(Z_6^2 - 2Z_8 Z_6 \cos(\theta_8 - \theta_6) + Z_8^2)$$

$$b = 4\,Z_{10}(Z_6 \sin\theta_6 - Z_8 \sin\theta_8)(Z_6^2 - 2Z_8 Z_6 \cos(\theta_8 - \theta_6) + Z_8^2 + Z_{10}^2 - Z_9^2)$$

$$c = (Z_6^2 - 2Z_8 Z_6 \cos(\theta_8 - \theta_6) + Z_8^2 + Z_{10}^2 - Z_9^2)^2 - 4Z_{10}^2(Z_6^2 \cos^2\theta_6 - 2Z_8 Z_6 \cos\theta_8 \cos\theta_6 + Z_8^2 \cos^2\theta_8)$$

$$\theta_{10} = \sin^{-1}\left[\frac{-b \pm \sqrt{b^2 - 4ac}}{2a}\right] \tag{3.38}$$

$$\theta_9 = \cos^{-1}\left[\frac{Z_6 \cos\theta_6 - Z_8 \cos\theta_8 + Z_{10} \cos\theta_{10}}{Z_9}\right] \tag{3.39}$$

Angular Velocity Analysis:

The derivation for the velocity and acceleration will differ from the rest since all four links are mobile. Taking the time derivative of eq. (3.37) gives the equation describing the velocity of Loop 3:

$$\dot{\theta}_8 i Z_8 e^{i\theta_8} + \dot{\theta}_9 i Z_9 e^{i\theta_9} = \dot{\theta}_6 i Z_6 e^{i\theta_6} + \dot{\theta}_{10} i Z_{10} e^{i\theta_{10}} \tag{3.40}$$

Separating eq. (3.40) into its imaginary and real components, the unknown velocities can be solved giving the following:

$$\dot{\theta}_9 = \frac{\dot{\theta}_6 Z_6 \sin\theta_6 + \tan\theta_{10}\left(\dot{\theta}_8 Z_8 \cos\theta_8 - \dot{\theta}_6 Z_6 \cos\theta_6\right) - \dot{\theta}_8 Z_8 \sin\theta_8}{Z_9(\sin\theta_{10} - \cos\theta_9 \tan\theta_{10})} \tag{3.41}$$

With the solution to the velocity of link Z_9 the velocity of link Z_{10} can be solved:

$$\dot{\theta}_{10} = \frac{\dot{\theta}_8 Z_8 \cos\theta_8 - \dot{\theta}_6 Z_6 \cos\theta_6 + \dot{\theta}_9 Z_9 \cos\theta_9}{Z_{10}\cos\theta_{10}} \tag{3.42}$$

Acceleration Analysis:

Taking the time derivative of eq. (3.40) gives the equation describing the acceleration of loop 3:

$$\begin{aligned} Z_8\left(-\dot{\theta}_8^2 + \ddot{\theta}_8 i\right)e^{i\theta_8} + Z_9\left(-\dot{\theta}_9^2 + \ddot{\theta}_9 i\right)e^{i\theta_9} \\ = Z_6\left(-\dot{\theta}_6^2 + \ddot{\theta}_6 i\right)e^{i\theta_6} + Z_{10}\left(-\dot{\theta}_{10}^2 + \ddot{\theta}_{10} i\right)e^{i\theta_{10}} \end{aligned} \tag{3.43}$$

Separating eq. (3.43) into its imaginary and real components, the unknown accelerations can be solved giving the following:

$$\ddot{\theta}_{10} = \frac{B\tan\theta_9 - A}{Z_{10}(\sin\theta_{10} - \cos\theta_{10}\tan\theta_9)} \tag{3.44}$$

$$\ddot{\theta}_9 = \frac{B + Z_{10}\ddot{\theta}_{10}\cos\theta_{10}}{Z_9\cos\theta_9} \tag{3.45}$$

$$A = Z_6\left(\dot{\theta}_6^2\cos\theta_6 + \ddot{\theta}_6\sin\theta_6\right) + Z_{10}\dot{\theta}_{10}^2\cos\theta_{10} - Z_8\left(\dot{\theta}_8^2\cos\theta_8 + \ddot{\theta}_8\sin\theta_8\right) - Z_9\dot{\theta}_9^2\cos\theta_9 \tag{3.46}$$

$$B = Z_6\left(-\dot{\theta}_6^2\sin\theta_6 + \ddot{\theta}_6\cos\theta_6\right) - Z_{10}\dot{\theta}_{10}^2\sin\theta_{10} - Z_8\left(-\dot{\theta}_8^2\sin\theta_8 + \ddot{\theta}_8\cos\theta_8\right) + Z_9\dot{\theta}_9^2\sin\theta_9 \tag{3.47}$$

where A and B represents the known variables in the equation.

3.3 Dynamic Analysis

The most critical step involved with the calculation of the energy is the dynamics, which is used to calculate the torque needed to turn the crank at a specified velocity and acceleration. It also returns all the joint forces in the leg mechanism. To perform the dynamic analysis some assumptions need to be made. Furthermore, generic dynamic equations can be formulated for the binary and tertiary link. Then using these equations the dynamic equations can be derived for each link.

3.3.1 Dynamic Assumptions

As mentioned earlier, certain assumptions need to be formulated to perform the dynamic analysis. The assumptions made for the system are:

1) The links are rigid.

2) The friction in the joints are ignored.

3) It is assumed that the hip of leg mechanism will be travelling at a constant velocity. Therefore, I use the assumption that the leg is hanging from a frame, where any acceleration effects of the moving frame is ignored.

4) When the leg comes into contact with the ground it is assumed to have zero impact.

5) When there is a rapid change in the torque at the crank it is assumed that the motor driving the crank is strong enough to overcome it and continue to drive the crank at a constant angular velocity.

6) To estimate the x component of force acting between the foot and the ground I examined the leg mechanism as a whole instead of each link separately. Furthermore, I analyzed the foot of the leg as having zero slip along the ground. In this case the mass of the hip moving forward is considered to be the amount that each leg would support, which is the weight of two leg mechanisms. Furthermore, the relative acceleration between the frame and the foot can be calculated. For the case of the stationary foot, this acceleration would approximately be the acceleration that the center of gravity of the leg mechanism would experience. Therefore, the x component of force would be equal to the amount of traction force needed to accelerate the center of mass forward at the calculated foot acceleration.

7) The y component of force is defined as the amount of force needed to provide the necessary amount of friction to counteract the x component of the force seen at the foot.

As mentioned previously, when the foot is in contact with the ground there are too many unknowns than equations. In total, the dynamics will return 21 linear equations with 23 unknowns, where two of the unknowns are the reaction forces on the ground. As a result, assumptions need to be formulated to estimate these forces. Assumption 6 and 7 that

were mentioned prior, are my assumptions used to estimate these forces. Furthermore, the forces at the foot become zero when the foot lifts off the ground.

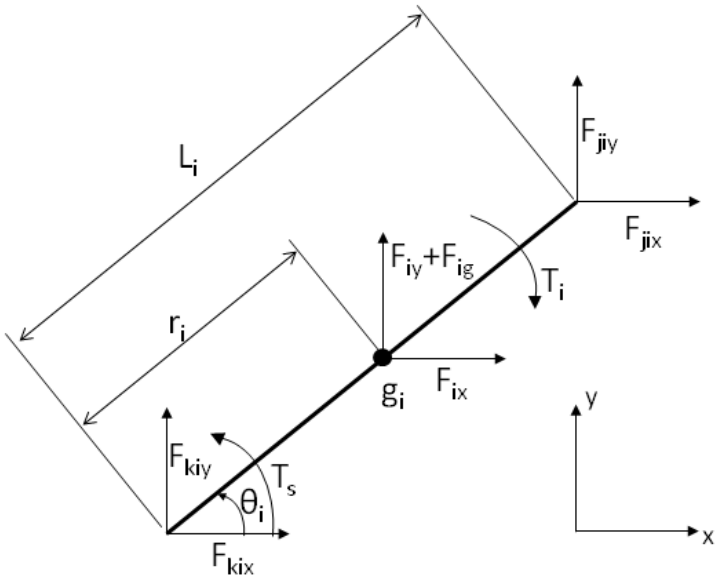

Figure 3.4: Free Body Diagram a Binary Link

3.3.2 General Dynamic Equations

The derivation of the dynamic equations is performed with the use of the superposition method [22, pg. 321-329], where the derived equations are linear in the inertia forces. The leg mechanism is broken down into individual free body diagrams for each link, and then they are superimposed to represent the total system. The free body diagram returns three equations for each link. There are two different links used in the leg mechanism, one is the binary link and the other is the tertiary link. General equations were formed for each type of link. Figure 3.4 shows the free body diagram of a binary link, where three linear equations can be derived. These are the summation of the x and y component of

forces is equal to zero, and the sum of the moment about the center of gravity (g_i) is equal to zero. Summing the x-component of forces gives:

$$\sum F_x = 0 = \sum_{j_1}^{j_n} F_{jix} + \sum_{k_1}^{k_2} F_{kix} + F_{ix} \tag{3.48}$$

where the subscript *i* is the number of the link, k and j are an array (ex: $j=[j_1, j_2 \ldots j_{n-1}, j_n]$) containing the number of each link attached to the corresponding end of the link. Therefore, the summation begins with the first number (j_1 and k_1) in the array and continues until the last number (j_n and k_n) is used. F_{ji} and F_{ki} are the reaction forces between the attached links where F_{ji}=-F_{ij}. F_{ig} is the gravitational force of the mass of the link (m_i) acting at the center of gravity (g_i), and F_i is the linear inertia forces acting at the center of gravity where F_i is described as:

$$F_i = -A_{gi} m_i e^{i\theta_{Ai}} \tag{3.49}$$

where A_{gi} and θ_{Ai} is the magnitude and direction of the linear acceleration at g_i. Separating eq. (3.49) into its x and y-components gives:

$$F_{ix} = -A_{gi} m_i \cos\theta_{Ai} \quad \text{and} \quad F_{iy} = -A_{gi} m_i \sin\theta_{Ai} \tag{3.50}$$

Summing the y-component of forces gives:

$$\sum F_y = 0 = \sum_{j_1}^{j_n} F_{jiy} + \sum_{k_1}^{k_2} F_{kiy} + F_{iy} + F_{ig} \tag{3.51}$$

Taking the summation of the moments about the center of gravity gives:

$$\sum M = 0 = T_i + T_s + r_i \sum_{k_1}^{k_n} \left[F_{kix} \sin\theta_i - F_{kiy} \cos\theta_i\right] + (1 - r_i) \sum_{j_1}^{j_n} \left[-F_{jix} \sin\theta_i + F_{jiy} \cos\theta_i\right] \tag{3.52}$$

where r_i is the distance from one end of the link to the center of mass (g_i – Figure 3.4). T_s is the torque exerted on the link from an attached shaft and T_i is the rotational inertia, which can be seen as:

$$T_i = -I_{gi}\alpha_i \tag{3.53}$$

where I_{gi} is the inertia about the center of gravity and α_i is the angular acceleration of the link.

The second type of link seen on the leg mechanism is the tertiary link seen in Figure 3.5. The link differs in the sense that the center of gravity is not conveniently located along a link, thus it is necessary to find its location along with the lengths r_i, C_i, D_i and angles $\tilde{\phi}_i, \tilde{\psi}_i$ and $\tilde{\beta}_i$ as seen in Figure 3.5. Again three equations can be derived and are shown as follows:

$$\sum F_x = 0 = \sum_{j_1}^{j_n} F_{jix} + \sum_{k_1}^{k_2} F_{kix} + \sum_{l_1}^{l_n} F_{lix} + F_{ix} \tag{3.54}$$

$$\sum F_y = 0 = \sum_{j_1}^{j_n} F_{jiy} + \sum_{k_1}^{k_2} F_{kiy} + \sum_{l_1}^{l_n} F_{liy} + F_{iy} + F_{ig} \tag{3.55}$$

$$\sum M = 0 = T_i + r_i \sum_{j_1}^{j_n} \left[F_{jix} \sin\tilde{\phi}_i - F_{jiy} \cos\tilde{\phi}_i\right]$$

$$+ D_i \sum_{k_1}^{k_n} \left[-F_{kix} \sin\tilde{\beta}_i + F_{kiy} \cos\tilde{\beta}_i\right] \tag{3.56}$$

$$+ C_i \sum_{l_1}^{l_n} \left[-F_{lix} \sin\tilde{\psi}_i + F_{liy} \cos\tilde{\psi}_i\right]$$

These general equations can then be applied to each link of the leg mechanism to get the dynamic equations describing the entire system.

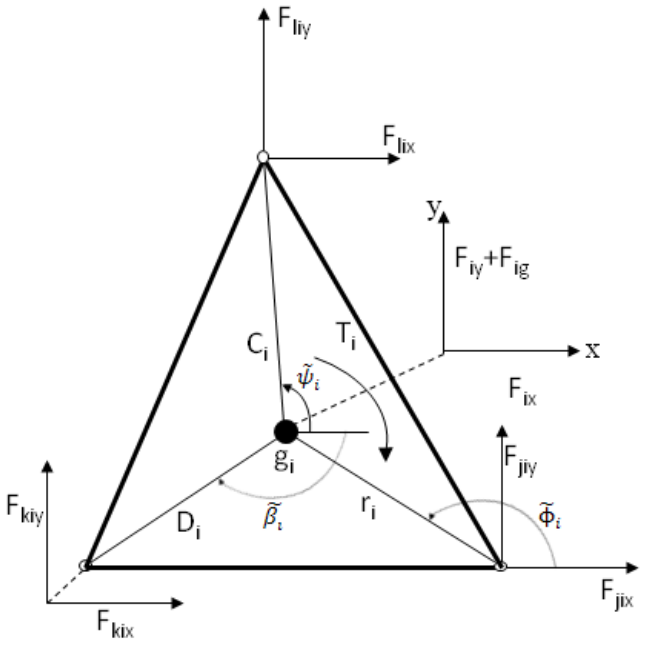

Figure 3.5: Free Body Diagram a Tertiary Link

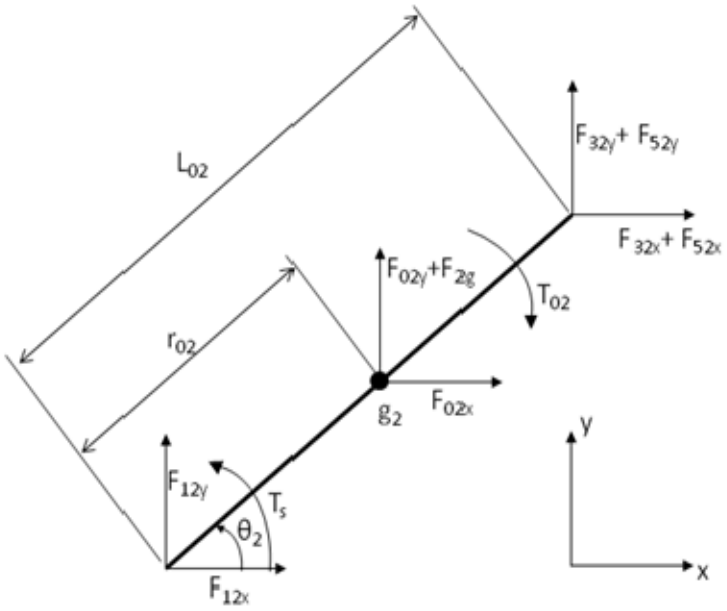

Figure 3.6: Free Body Diagram, Link Z_2

3.3.3 Dynamic Equations

The following gives detailed derivations of each link. These include the free body diagram showing the forces acting on each link. These equations are derived using the general equations described in Section 3.3.2.

Dynamics of Link Z_2 (Figure 3.6)

Summing the forces:

$$\sum F = 0 = F_{02} + F_{12} + F_{32} + F_{52} + F_{2gy}$$

Separating into the x and y-components of force yields with the known constants on the left of the equal sign:

$$F_{02x} = -F_{12x} + F_{23x} + F_{25x} \tag{3.56}$$

$$F_{02y} + F_{2gy} = -F_{12y} + F_{23y} + F_{25y} \tag{3.57}$$

Summing the moment about the center of mass (Counter clockwise moment is positive) with the known constants on the left of the equal sign:

$$\sum M = 0 = T_{02} + r_{02}(F_{12x}\sin\theta_2 - F_{12y}\cos\theta_2) + (L_{02} - r_{02})(-F_{32x}\sin\theta_2 + F_{32y}\cos\theta_2 - F_{52x}\sin\theta_2 + F_{52y}\cos\theta_2) + T_s$$

Rearranging:

$$T_{02} = r_{02}\left(-F_{12x}\sin\theta_2 + F_{12y}\cos\theta_2\right) + (L_{02} - r_{02})(-F_{23x}\sin\theta_2 + F_{23y}\cos\theta_2 - F_{25x}R_{02}\sin\theta_2 + F_{25y}\cos\theta_2) + T_s \tag{3.58}$$

Dynamics of Link Z_3 (Figure 3.7)

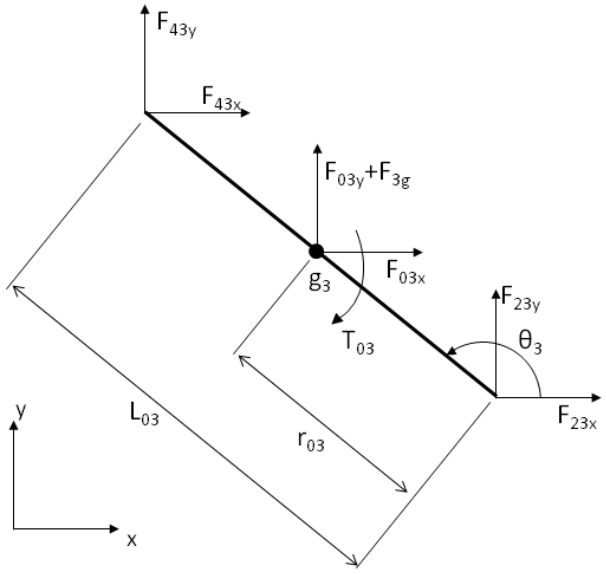

Figure 3.7: Free Body Diagram, Link Z_3

Summing the forces:

$$\sum F = 0 = F_{03} + F_{23} + F_{43} + F_{3g}$$

Separating into the x and y-components of force yields with the known constants on the left of the equal sign:

$$F_{03x} = -F_{23x} + F_{34x} \tag{3.59}$$

$$F_{03y} + F_{3gy} = -F_{23y} + F_{34y} \tag{3.60}$$

Summing the moment about the center of mass with the known constants on the left of the equal sign:

$$\sum M = 0 = T_{03} + r_{03}\left(F_{23x}\sin\theta_3 - F_{23y}\cos\theta_3\right) + (L_{03} - r_{03})(-F_{43x}\sin\theta_3 + F_{43y}\cos\theta_3)$$

Rearranging:

$$T_{03} = r_{03}\left(-F_{23x}\sin\theta_3 + F_{23y}\cos\theta_3\right) + (L_{03} - r_{03})(-F_{34x}\sin\theta_3 + F_{34y}\cos\theta_3) \tag{3.61}$$

Dynamics of Link $Z_4Z_7Z_8$ (Figure 3.8)

Summing the forces:

$$\sum F = 0 = F_{04} + F_{14} + F_{34} + F_{94} + F_{4gy}$$

Separating into the x and y-components of force yields with the known constants on the left of the equal sign:

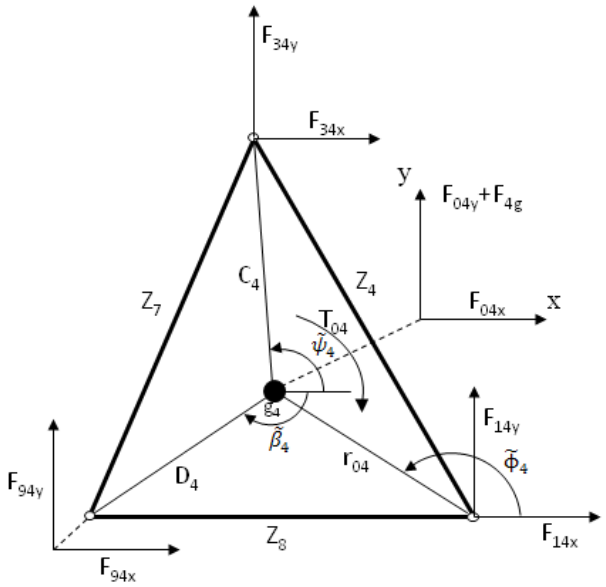

Figure 3.8: Free Body Diagram, Link $Z_4Z_7Z_8$

$$F_{04x} = -F_{14x} - F_{34x} + F_{49x} \tag{3.62}$$

$$F_{04y} + F_{4gy} = -F_{14y} - F_{34y} + F_{49y} \tag{3.63}$$

Summing the moment about the center of mass with the known constants on the left of the equal sign:

$$\sum M = 0 =$$

$$T_{04} + r_{04}(F_{14x}\sin\tilde{\phi}_4 - F_{14y}\cos\tilde{\phi}_4) + C_4(-F_{34x}\sin\tilde{\Psi}_4 +$$

$$F_{34y}\cos\tilde{\Psi}_3) + D_4(-F_{94x}\sin\tilde{\beta}_4 + F_{94y}\cos\tilde{\beta}_4)$$

Rearranging:

$$T_{04} = r_{04}(-F_{14x}\sin\tilde{\phi}_4 + F_{14y}\cos\tilde{\phi}_4) + C_4(F_{34x}\sin\tilde{\Psi}_4 - F_{34y}\cos\tilde{\Psi}_4) + D_4(-F_{49x}\sin\tilde{\beta}_4 + F_{49y}\cos\tilde{\beta}_4) \tag{3.64}$$

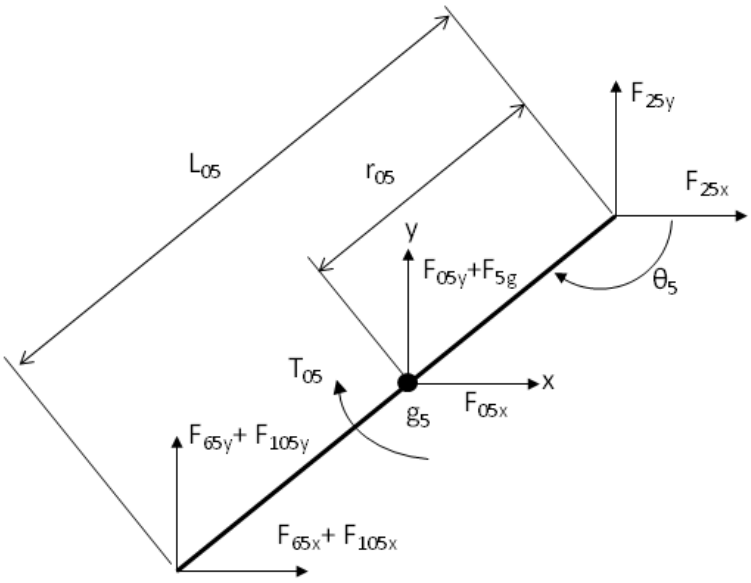

Figure 3.9: Free Body Diagram, Link Z_5

Dynamics of Link Z_5 (Figure 3.9)

Summing the forces:

$$\sum F = 0 = F_{05} + F_{25} + F_{65} + F_{105} + F_{5gy}$$

Separating into the x and y-components of force yields with the known constants on the left of the equal sign:

$$F_{05x} = -F_{25x} + F_{56x} + F_{510x} \tag{3.65}$$

$$F_{05y} + F_{5gy} = -F_{25y} + F_{56y} + F_{510y} \tag{3.66}$$

Summing the moment about the center of mass with the known constants on the left of the equal sign:

$$\sum M = 0 = T_{05} + r_{05}(F_{25x}\sin\theta_5 - F_{25y}\cos\theta_5) + (L_{05} -$$

$$r_{05})(-F_{65x}\sin\theta_5 + F_{65y}\cos\theta_5 - F_{105x}\sin\theta_5 + F_{105y}\cos\theta_5)$$

Rearranging:

$$T_{05} = r_{05}(-F_{25x}\sin\theta_5 + F_{25y}\cos\theta_5) + (L_{05} - r_{05})$$
$$(-F_{56x}\sin\theta_5 + F_{56y}\cos\theta_5 - F_{510x}\sin\theta_5 + F_{510y}\cos\theta_5) \quad (3.67)$$

Dynamics of Link Z_6 (Figure 3.10)

Summing the forces:

$$\sum F = 0 = F_{06} + F_{16} + F_{56} + F_{6g}$$

Separating into the x and y-components of force yields with the known constants on the left of the equal sign:

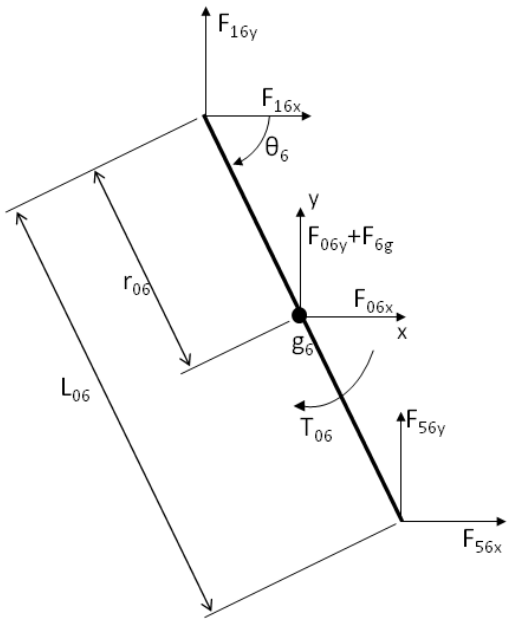

Figure 3.10: Free Body Diagram, Link Z_6

$$F_{06x} = -F_{16x} - F_{56x} \tag{3.68}$$

$$F_{06y} + F_{6gy} = -F_{16y} - F_{56y} \tag{3.69}$$

Summing the moment about the center of mass with the known constants on the left of the equal sign:

$$\sum M = 0 = T_{06} + r_{06}(F_{16x}\sin\theta_6 - F_{16y}\cos\theta_6) + (L_{06} - r_{06})(-F_{56x}\sin\theta_6 + F_{56y}\cos\theta_6)$$

Rearranging:

$$T_{06} = r_{06}(-F_{16x}\sin\theta_6 + F_{16y}\cos\theta_6) + (L_{06} - r_{06})(F_{56x}\sin\theta_6 - F_{56y}\cos\theta_6) \tag{3.70}$$

Dynamics of Link Z_9 (Figure 3.11)

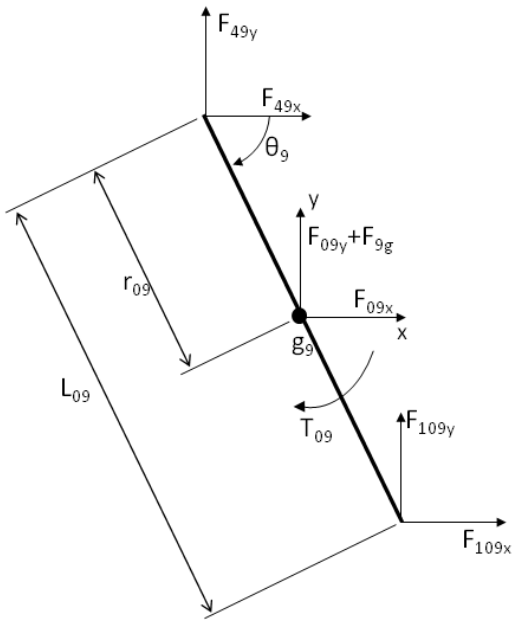

Figure 3.11: Free Body Diagram, Link Z_9

Summing the forces:

$$\sum F = 0 = F_{09} + F_{49} + F_{109} + F_{9g}$$

Separating into the x and y-components of force yields with the known constants on the left of the equal sign:

$$F_{09x} = -F_{49x} + F_{910x} \tag{3.71}$$

$$F_{09y} + F_{9gy} = -F_{49y} + F_{910y} \tag{3.72}$$

Summing the moment about the center of mass (Counter clockwise moment is positive) with the known constants on the left of the equal sign:

$$\sum M = 0 = T_{09} + r_{09}(F_{49x}\sin\theta_9 - F_{49y}\cos\theta_9) + (L_{09} - r_{09})(-F_{109x}\sin\theta_9 + F_{109y}\cos\theta_9)$$

Rearranging:

$$T_{09} = r_{09}(-F_{49x}\sin\theta_9 + F_{49y}\cos\theta_9) + (L_{09} - r_{09})(-F_{910x}\sin\theta_9 + F_{910y}\cos\theta_9) \tag{3.73}$$

Dynamics of Coupler $Z_{10}Z_{11}Z_{12}$ (Figure 3.12)

Summing the forces:

$$\sum F = 0 = F_{10} + F_{510} + F_{910} + F_L + F_{10gy}$$

Separating into the x and y-components of force yields with the known constants on the left of the equal sign:

$$F_{10x} + F_{Lx} = -F_{510x} - F_{910x} \tag{3.74}$$

$$F_{10y} + F_{10gy} + F_{Ly} = -F_{510y} - F_{910y} \tag{3.75}$$

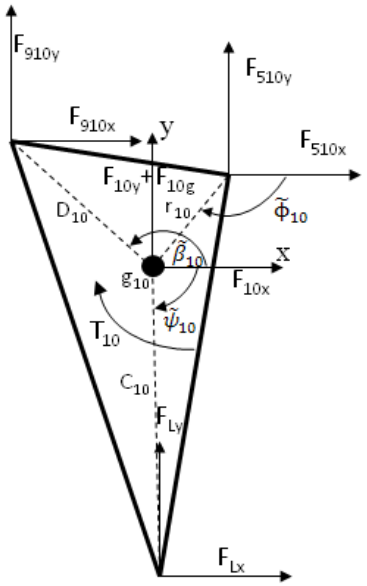

Figure 3.12: Free Body Diagram, Link $Z_{10}Z_{11}Z_{12}$

Summing the moment about the center of mass (Counter clockwise moment is positive) with the known constants on the left of the equal sign:

$$\sum M = 0 =$$

$$T_{10} + C_{10}(-F_{Lx}\sin\tilde{\psi}_{10} + F_{Ly}\cos\tilde{\psi}_{10}) + r_{10}(F_{510x}\sin\tilde{\phi}_{10} -$$

$$F_{510y}\cos\tilde{\phi}_{10}) + D_{10}(-F_{910x}\sin\tilde{\beta}_{10} + F_{910y}\cos\tilde{\beta}_{10})$$

Rearranging:

$$T_{10} + C_{10}(-F_{Lx}\sin\tilde{\psi}_{10} + F_{Ly}\cos\tilde{\psi}_{10}) = r_{10}(-F_{510x}\sin\tilde{\phi}_{10} + F_{510y}\cos\tilde{\phi}_{10}) + D_{10}(F_{910x}\sin\tilde{\beta}_{10} - F_{910y}\cos\tilde{\beta}_{10}) \tag{3.76}$$

There are two comments regarding the dynamic equations. First, when examining link Z_2, the forces exerted by link Z_3 and Z_5 act directly on link Z_2 and not directly upon each

other. However, they still do have an impact on each other because the effect between the two links is accounted for in the equations for link Z_2. The same occurs for link Z_5 where it attaches to link Z_6 and Z_{10}. The forces of link Z_6 and Z_{10} act through link Z_5 and not directly upon each other. (Note: Link 1 is considered to be the frame of the leg, hence F_{12} is the reaction force between the frame (ground) and Z_2.)

3.4 Summary

The analysis methods in this chapter are extremely important in improving the performance of the leg mechanism. The derivation of all the kinematic information gives the ability to check the constraints and the initial success of the leg mechanism. The second portion which depends on the kinematic solutions is the dynamic equations. These dynamic equations take into account the inertia forces of the rotating links, something that is not seen in previous work. The dynamics gives insight into the energy and efficiency of the leg mechanism. More importantly, with the ability to calculate the dynamics and energy, it is possible to optimize the mechanism to lower the amount of energy used. The optimization of this energy is discussed in the next chapter. Furthermore, the dynamic equations give lots of insightful information regarding all the reaction forces between links, as well as the driving torque needed on the crank to drive at a specified speed and acceleration of the crank.

Chapter 4

4. Optimization

4.1 Introduction

Optimization techniques are a widely used tool applicable to a wide range of problems. Currently many techniques and programs exist which creates an easy user interface to set up and run an optimization for a given problem. Depending on the problem, there can be many additions to the problem to satisfy numerous criteria, such as constraints, the search range of the variables, etc. This thesis is an optimization problem that needs to satisfy imposed constraints on the design. One difficulty is that optimizations usually depend on how the problem is set up and what choices are made in terms of the objective functions and constraints.

This chapter is organized as follows; the first section discusses the objective functions that will be utilized for this problem, and the second section discusses any additional constraints that are needed for the problem.

4.2. Objective Functions

In every optimization there always needs to be goals and objectives that the optimization strives to achieve. These can be single or multi objective problems. However, the

addition of extra objectives increases the difficulty of finding the optimized solution, because in many cases a change that improves one objective can decrease another. Furthermore, the objective function can be very difficult to choose because some objectives will return very poor results while others can be very efficient. A great deal of thought needs to be put into each objective to try and possibly predict its effect on the overall problem.

Initially the only objective that was considered was the minimization of the energy in the system. When I thought about what would occur during the optimization it came to mind that it would most likely move towards a smaller foot path that required minimal movement of the links. This prediction was made because a system that makes minimal movements would most likely require less energy than a system with a larger path and one where the links move through a greater range of angles. To overcome this predicted trend, the maximization of the stride length was added to the optimization problem. As a result, in this section three separate objectives are discussed for this specific problem. First is a very important objective which is the minimization of energy, second is the maximization of the stride length, and third is the combination of the two objectives to create one objective for convenience purposes when using the Matlab software.

4.2.1 Objective One: Minimizing the Energy

The first objective of the optimization is the minimization of the energy over the cycle. This is calculated by integrating the torque squared over the complete cycle of the crank. To do this, the analysis techniques described in Chapter 3 are used. With the known

information of the links (mass, location of the center of mass, etc), the kinematic information of the crank, and the forces acting on the foot, the 21 linear equations can be solved to find the reaction forces acting at the joints, as well as the torque being applied to the crank. The torque is then found at each small increment of the crank to find the torque profile. One area of caution is the step increment of the crank, because if the increment is too large then the integral of the torque squared will have some errors when compared to a very fine increment. A very fine increment is not used because it requires a greater amount of computational time. Therefore, an increment was used that had minimal error when compared to the fine increment, yet it is still computationally quick. The integral of the torque squared over the cycle is seen in the following:

$$O1: = \int_0^{\tau} T^2 dt \tag{4.1}$$

where τ is the amount of time it takes to complete a full rotation of the crank and T is the torque being applied to the crank.

4.2.2. Objective Two: Maximizing the Stride Length

In legged locomotion the stride length per cycle is important along with the energy consumption. The stride length is calculated by calculating the displacement of the foot. Two extremities are found where the leg leaves and makes contact with the ground. The equations for calculating the positions of the footpath (Figure 4.1) are:

$$Y\_POS = Z_6 \sin\theta_6 + Z_{12} \sin(\theta_{12}) \tag{4.2}$$

$$X\_POS = Z_6\cos\theta_6 + Z_{12}\cos(\theta_{12}) \tag{4.3}$$

Since the foot path between the two extremities is flat, the stride length is approximated by the horizontal distance between the two points (Figure 2.1b) seen as:

$$O2 := |F_1 - F_2| \tag{4.4}$$

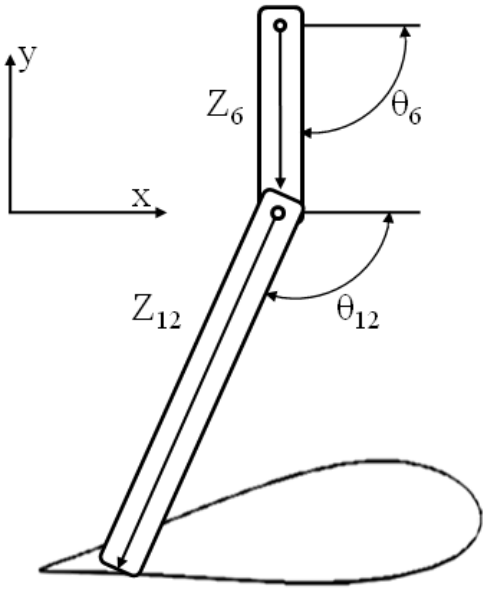

Figure 4.1: Foot Path Calculation

4.2.3. Objective Three: Combination of objectives

For convenience purposes a single objective was created because it is much easier to set up the Matlab software for one objective. I decided to combine the two objective functions to create a single objective. The combined objective was decided to be a minimization problem. This was done by dividing objective one by objective two because it is more applicable to examine how much energy is used for a travelled distance. In other words I calculate the energy used per unit of travel:

$$03 := \frac{\int_0^{\tau} T^2 dt}{|F_1 - F_2|} \tag{4.5}$$

Therefore, as the step length increases the objective function will decrease.

4.3 Constraints Functions-Maximum Foot Force

The optimization uses the same constraints as previously discussed in Section 2.4, however there is one additional constraint that is added to the optimization problem. The reaction force on the foot is bounded by the mass of the leg. The maximum amount of force in the x-component (F_{Lx}) of the force is equal to the maximum amount of mass that the foot would support times the coefficient of friction. If the x-component of force exceeds this amount then the solution is rejected.

$$C9 := F_{Lx} \leq F_{Lymax} * \mu_{friction} \tag{4.6}$$

where F_{Lymax} is the maximum possible force that can be experienced at the foot which would be the force needed to support two times the mass of a leg, and $\mu_{friction}$ is the coefficient of friction.

4.4 Optimization Program

Matlab optimization toolbox was used to perform the optimization. The program was setup to operate in the following manner. First, the variables of the optimization as discussed in Section 5.3 are defined. Next, the first stage of the design is performed, which is the design of the four-bar mechanism ($Z_1Z_2Z_3Z_4$ and $Z_1Z_2Z_5Z_6$, Figure 2.2) and

the free choice of θ_c and Z_8 are defined. The constraints C1 and C2 are then verified to ensure that the four-bar is a crank rocker. Next the second stage of the design is performed. During this portion of the design, the constraints C7 and C8 are minimized to ensure the solution does not violate the first stage of the design and to try and force the mechanism $Z_6Z_8Z_9Z_{10}$ (Figure 2.2) to perform as a parallel mechanism, however it is only preferred and is not necessary that it behaves in this manner. Following the complete design of the leg configuration, the constraints C3, C4, C5 and C6 are examined to verify if the foot path behaves in a desirable manner, and to monitor the behaviour of $Z_6Z_8Z_9Z_{10}$ mechanism. If all the constraints are satisfied, then the complete kinematics of each link is calculated followed by the calculation of the dynamics of the leg mechanism. With the dynamics, the objective function eq. (4.5) is calculated to numerically define the performance of the leg design. Then the optimization software changes the variables based on this result and the process is repeated.

4.5 Summary

The optimization described in this section is critical to the improvement of the leg mechanism. The addition of setting certain variables as constants creates a more feasible optimization problem. The most critical aspect of the optimization is the defined objective functions because the success of the optimization is based on these objectives. This problem contains two main focuses of optimization, which is the reduction of energy used during a cycle and the maximization of the step length. By optimizing these two

aspects it is believed that the final mechanism will be more efficient in terms of energy and will maintain an acceptable foot path while improving on the step length.

Chapter 5

5. Results and Discussion

5.1 Introduction

To evaluate the success of the optimization, the optimized results are compared to trial-and-error results that were achieved prior to the application of the optimization process. While performing the trial-and-error calculations there was a different goal being pursued. The main goal was to achieve a foot tracer path that had a long flat profile while maintaining a continuous foot path with a valid mechanism that can operate through a full crank rotation. The goal of the optimization was to show that these results can be greatly improved with the use of mechanism design, and the energy and dynamics of the system. However, like many multi objective optimization problems there is usually a compromise between the successes of each objective.

5.2 Trial-and-Error Results

The trial-and-error portion was performed by changing variables and examining how it affects the mechanism tracer path and then making a judgement on which variables to change for the next iteration of the process. The variables changed during these iterations are the ones discussed in Section 2.3.4. After a substantial amount of time an excellent looking mechanism and tracer path was found. For the constraints imposed on the system

a minimum stride length (HC1) of 9 cm was chosen. All the angles within the corners of the parallel mechanism ($Z_6Z_8Z_9Z_{10}$, Figure 2.2) needs to be between 5° (HC2) and 175° (HC3), and the vertical offset (HC4) used to define the stride length was set at 0.002m. For the best achieved result, the function that was used for the function generator was, $y = 30° sin(x - 65°) + 105°$. With this function the free choice of the ground spacing Z_1 was chosen to be 15cm and the desired range of the input link (φ) and the output link (ψ) are chosen to have a one to one relationship with the equation, therefore $\varphi_i=x_i$ and $\psi_i=y_i$. This was chosen to eliminate four of the free choices which are the desired ranges of the input and output links. As a note, the ground spacing was kept the same throughout the trial-and-error analysis to eliminate any scaling effects. Furthermore, the four-bar component $Z_1Z_2Z_3Z_4$ was chosen to be identical to $Z_1Z_2Z_5Z_6$ (Figure 2.2) because then the function generator is only performed once, thus lowering the free choices, where good results were still obtained. Next, a coupler angle of 60° was chosen for θ_c and a length of 10cm was chosen for Z_8. For the second stage of the design a length of 19cm was chosen for the length of Z_{12}, and the chosen leg angles at the four precision points are -98°, -102°, -74° and -46°.

The results using these free choices can be seen in Table 5.1 which lists the lengths of the links of the trial-and-error mechanism. Looking at how well the mechanism satisfied the constraints it was found that the stride length (F_1F_2 – Figure 2.1b) was 11.68cm. Further analysis shows that the highest obstacle that can be cleared (H – Figure 2.1b) is 6.5cm.

5.3 Optimization Results

To find the global optimal geometric design for the leg mechanism would be very computationally heavy and time consuming because the amount of variables becomes very large. However, a constrained multi-objective problem [27] simplifies the task making it more realistic to apply an optimization process. When performing the trial-and-error analysis certain trends were noticed where certain variables could be kept the same while finding many solutions. As a result, to simplify the problem some changes and steps used for the trial-and-error analysis are modified to reduce the computational time.

The first change involves the four-bar function generator, because there are currently five free choices involved with the synthesis of the four-bar. Instead I decided to have three free choices where I change the lengths Z_2, Z_3 and Z_4 while holding the ground spacing (Z_1) at a constant length throughout the optimization to exclude the effects of scaling. Modifying these three links changes the entire profile of the four-bar mechanism, therefore it is more efficient to have three changing parameters rather than five. The other remaining variables are the same as previously mentioned in Section 2.3. To simplify the problem some of the variables were set as constant values. During the trial-and-error search, preliminary results demonstrated that a crank angle range of 270° to 150° worked well for the region where the four precision points are contained. Chebyshev spacing [20, pg. 341-343] was used to calculate the values of θ_{2a}, θ_{2b}, θ_{2c}, θ_{2d} within the given range. Although Chebyshev spacing is used for function generation, good results were found with these crank directions and were chosen to be used for the remainder of the optimization process. When choosing the precision points there are endless possibilities and combinations for the locations of the four precision points used for the synthesis of

the mechanism. I found that I could find numerous solutions when I keep the angle of link Z_{12} at a constant value for each precision point. Therefore, the location of the precision points will differ based on the changing profile of the four-bar mechanisms and the length of Z_{12}. It was also found that when I kept the precision points in the same location, the amount of acceptable solutions were greatly reduced, thus giving reason to keeping the leg angles constant instead. With setting these variables to constant values the optimization problem is greatly reduced in complexity leaving a more realistic problem that uses 6 variables (Z_2, Z_3, Z_4, Z_8, Z_{12}, θ_c).

It is desired that a successful optimized solution will show a decrease in the amount of energy used as well as trying to increase the stride length. This problem has 6 variables as well as a short internal search to find the free choice β_2 (eq. (2.17) and eq. (2.19)) for both the dyad and the triad during the synthesis portion of the program. It was found that when looking at preliminary results for the optimization process that many local minimums exist over the search range. To ensure that this was true, trials were performed with different starting points as well as modifying the search ranges of each variable. In all cases, the problem of many local minimums was found. The possibility of using a genetic algorithm global optimization program was discussed, however it was decided that these techniques can sometimes be inconsistent and time consuming. Instead it was decided that finding the absolute maximum was not the main objective of the research. Therefore, a coarse exhaustive search was performed over a defined range for each variable. With the best found configurations I performed a local optimization at each of the results. I used fmincon (constrained non-linear minimization) toolbox for Matlab,

which can accept a large amount of variables with the ability to define certain constraints and regions of interest for each variable.

The goal of the optimization is to optimize or improve upon the initial trial-and-error design, where the focus was to achieve an acceptable foot profile that had a flat path along the ground. With the inclusion of minimizing the energy, improvements were seen with the very first optimization run. However, as stated prior local minimums were found.

Table 5.1: Trial-and-Error and Optimization Results

	Lengths	
Link Number	Trial-and-error	Optimized
Z_1	15 cm	15 cm
Z_2	4.17 cm	2.78 cm
Z_3	20.33 cm	20.02 cm
Z_4	12 cm	12.05 cm
Z_5	20.33 cm	20.02 cm
Z_6	12 cm	12.07 cm
Z_7	11.14 cm	12.30 cm
Z_8	10 cm	7.01 cm
Z_9	11.89 cm	12.08 cm
Z_{10}	10 cm	6.84 cm
Z_{11}	26.11 cm	22.31 cm
Z_{12}	19 cm	19.54 cm

For the optimization, the constraints were set as follows: a minimum stride length (HC1) of 10cm was chosen, all the angles within the corners of the parallel mechanism ($Z_6Z_8Z_9Z_{10}$) needs to be between 10° (HC2) and 170°, and the offset used to define the stride length was kept the same. The constraint values for the optimization were changed because with the software it was feasible to use greater restrictions than that of the trial-and-error situation.

When performing the calculations of the dynamics, the amount of data points has a large impact on the computational time needed. As a result, we used 400 data points and when compared to the use of 10000 data points there was 0.6% error with the calculated stride length and 0.05% with the calculated energy. This allows the calculations to finish with an acceptable amount of time and the error.

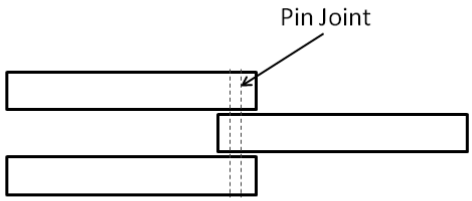

Figure 5.1: Pin Joint Layout for Two Attached Links

The leg angles for each precision point and the crank angle at each precision point are chosen to be the same as the solution found in the trial-and-error analysis. For the dynamic analysis the constants needed for these calculations need to be defined. However, some thought was needed with the mass of the links because a conceptual layout of the physical design needed to be considered. As a result, it was found that with pin joints a single link would have to be pinned to two identical links one on each side (Figure 5.1). This layout would prevent binding in the joint by balancing the force on each side of the single link. Following this layout certain links will be doubled in mass due to the necessity to prevent binding in the joints with a real prototype.

Therefore, the links Z_2, Z_3, Z_5, Z_6, Z_9 need to be doubled in mass while Z_4, Z_7, Z_8, Z_{10}, Z_{11} and Z_{12} remain the same. The remaining parameters that were chosen for the analysis are as follows: (i) the links are uniform with a density of 0.5 kg/m; (ii) a friction

coefficient of 0.5 is experienced between the foot and the ground; (iii) a constant crank velocity of 180°/sec (π rad/s); (iv) the length of Z_1 is kept constant for all designs to avoid any scaling effects. Furthermore, a set of legs are paired across from each other sharing the same crank, therefore with the assumption that one leg is in contact at all times then the leg will support a maximum of double the weight of a single leg, which comes into consideration when I calculate the x-force acting on the foot and the maximum possible traction force.

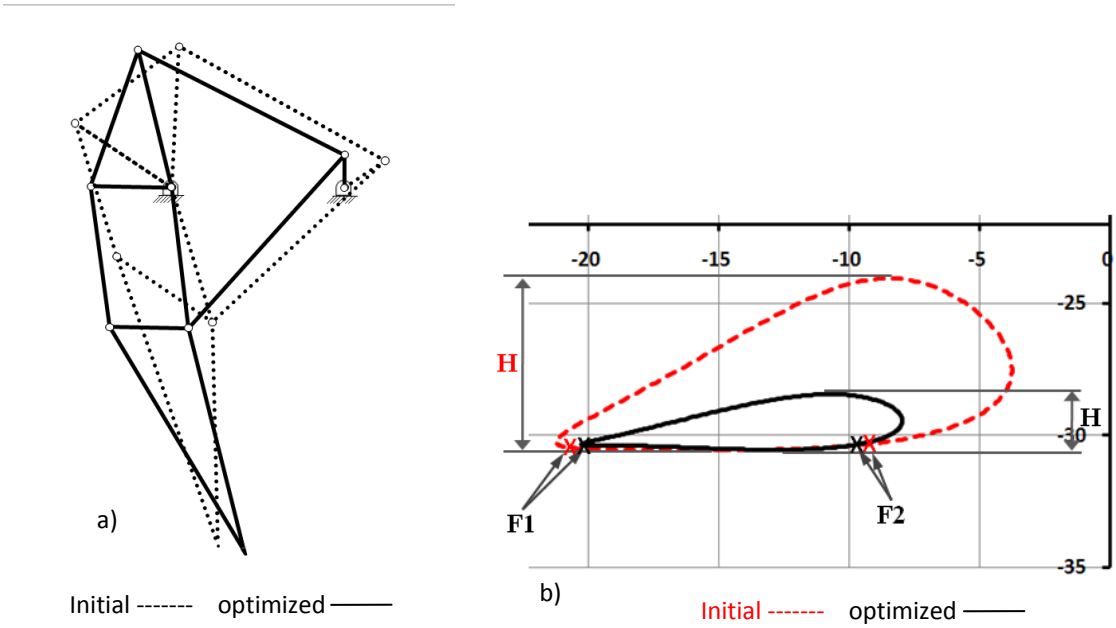

Figure 5.2: a) Comparison of Leg, b) Foot trajectories

With the application of the coarse exhaustive search with the optimization software being applied to the best results, substantial improvements on the objective functions and the mechanisms performance was obtained. Since large improvements were found, the optimization process was ended when the magnitude of improvements on the objective function are smaller than 10^{-6}. The results from the optimization can be seen in Table 5.1

with the results from the trial-and-error. Looking at the performance of the optimized model it had a stride length of 10.56cm. Further analysis shows that the highest obstacle that can be cleared is 2.11cm.

5.4 Comparison of Results

In Figure 5.2a the optimized (solid line) and the trial-and-error (dashed line) leg designs are shown demonstrating the difference in configurations. Some aspects of the leg had minor changes while others are very noticeable. The major differences are seen with the links Z_2, Z_8, Z_{10} and Z_{11}. It was expected that the length of Z_2 would be shorter because a smaller crank outputs more force for a given torque, therefore if the crank can be reduced in a system it would require less torque to provide the same magnitude of force at the tip. Figure 5.2b shows the foot trajectories of both designs. Notice that both designs have the similar flat profile along the ground. The big difference between the two trajectories is the return path. The optimized design's return path is shorter in height and in overall travel length, and thus less energy is used to overcome gravity and to move the links.

Some further speculations can be made when examining the kinematic analysis. Figure 5.3 to Figure 5.14 show the angle and velocity profiles of each link for the optimized (solid line) and the trial-and-error (dashed line) leg designs. When examining the angle profile of each link, the optimized solution's links have less amplitude of travel. The smaller amplitude indicates that the links will travel less distance, therefore less work is required. When examining the velocity profiles it was found that the amplitude of the optimized design was also less. Therefore, the acceleration of the link will be less as well,

which in return will indicate the inertia forces exerted on each link will be less for the optimized design. Although the change in inertia on each link might be small in magnitude, the contribution of each link added together can have a significant effect on the total amount of energy needed.

Figure 5.15 to Figure 5.34 shows the force reaction between connected links for the optimized (solid line) and the trial-and-error (dashed line) leg designs. The plots are separated into the x and y-components of force and each figure compares both designs. A general observation is that the optimized force profiles are for the most part lower in magnitude, which means there is less of a load on the joints and links, thus the crank has less force to overcome. However, some force profiles are very similar in magnitude, (Figures 5.26, 5.29, 5.30 and 5.34) thus showing minor improvements. When comparing the change in the x-component of forces to the y-component, it is found that the x-component profiles have experienced the most improvements between the two designs. However, when examining the x-component of force profiles it was seen that the largest improvements were found when the leg was off the ground. As a result, the forces due to the acceleration of the hip had less of an effect than the balancing and support of the links while off the ground.

Figure 5.35 shows the comparison of the torque profiles for the optimized (solid line) and the trial-and-error (dashed line) leg designs. When looking at this figure, the optimized solution is lower in magnitude where the largest improvements were achieved when the foot was off the ground. In the figure, there are two instances when there is a sudden change in the torque profile. This occurs because the analysis is examining a single leg and as a result it is assumed that when the leg is in the air the hip of the leg is stationary,

however when the leg comes into contact it suddenly accelerates the hip forward, giving the sudden change. In reality, the hip would be moving forward and when the foot comes into contact with the ground an analysis on the actual acceleration of the hip would need to be performed to calculate the sudden change in torque.

To compare the results of the optimization, the objective functions of the two designs are considered. When examining the overall objective function (O3) it was found that the optimized solution had a value of 0.01381N^2m·s. When examining the objective function representing the energy (O1) a value of 0.001455 N^2m^2·s was found. Examining the trial-and-error results it was found that the calculated overall objective function was 0.08597 N^2m·s, and that the objective function representing the energy was 0.01009 N^2m^2·s. When comparing the two design performances, the overall objective function of the optimized design was 84% less. Examining the overall energy of the system, the optimized solution decreased by 85.6%, and the stride length decreased by 10%. Although the decrease in energy was very desirable, the decrease in the stride length was not, however the magnitude of the decrease was not large. The reason for the decrease was due to the fact that the trial-and-error result had an excellent step length with high energy consumption. Therefore, the energy was the dominating factor in the optimization and thus overpowered the maximization of the stride length. Other aspects that improved are the peak torque of the optimized design that decreased by 55.4% and a peak joint force that decreased by 7.8% when compared to the initial design.

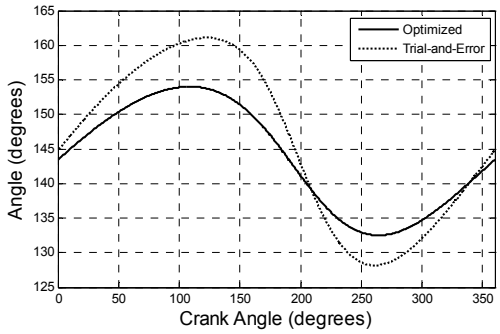

Figure 5.3: Angle of Link Z_3 vs. Crank Angle

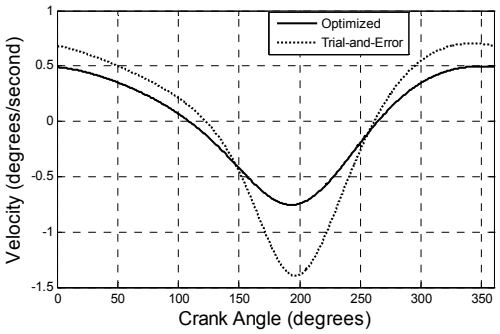

Figure 5.4: Velocity of Link Z_3 vs. Crank Angle

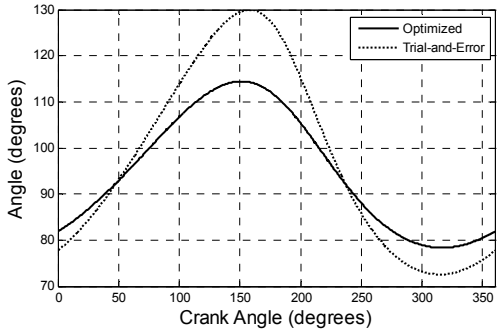

Figure 5.5: Angle of Link Z_4 vs. Crank Angle

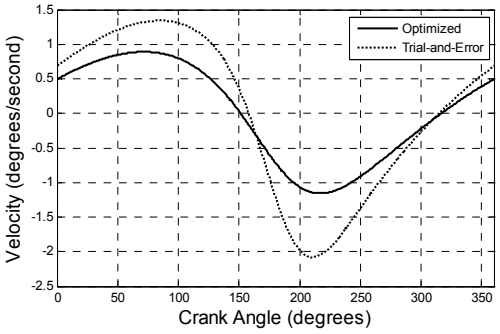

Figure 5.6: Velocity of Link Z_4 vs. Crank Angle

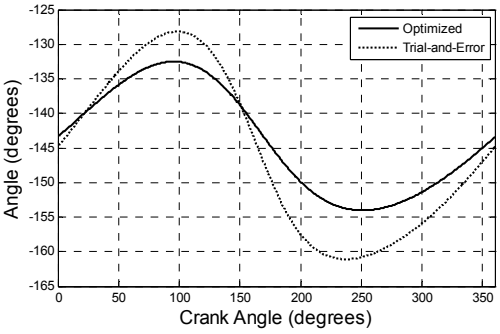

Figure 5.7: Angle of Link Z_5 vs. Crank Angle

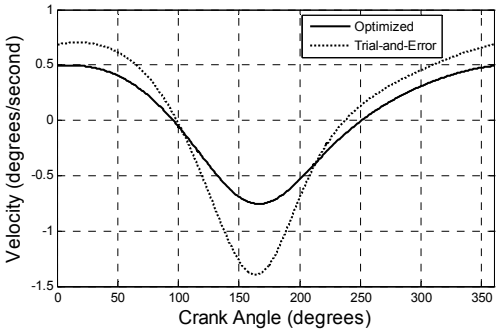

Figure 5.8: Velocity of Link Z_5 vs. Crank Angle

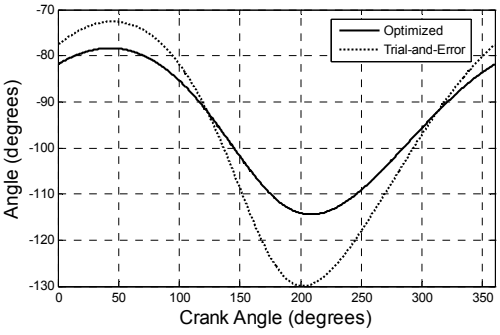

Figure 5.9: Angle of Link Z_6 vs. Crank Angle

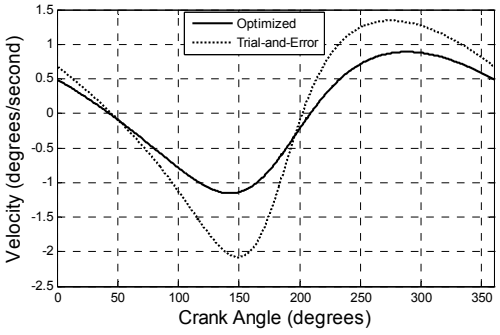

Figure 5.10: Velocity of Link Z_6 vs. Crank Angle

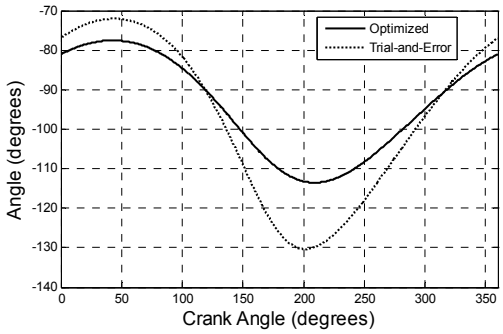

Figure 5.11: Angle of Link Z_9 vs. Crank Angle

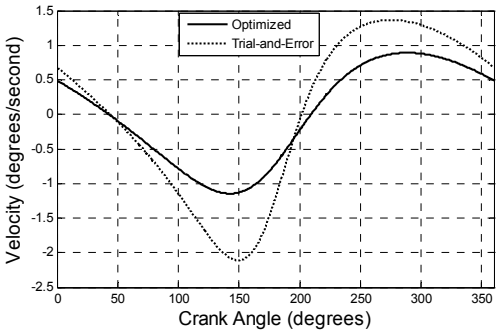

Figure 5.12: Velocity of Link Z_9 vs. Crank Angle

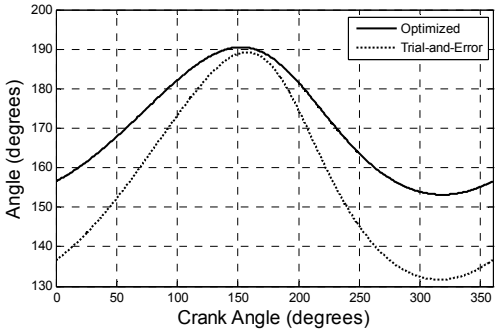

Figure 5.13: Angle of Link Z_{10} vs. Crank Angle

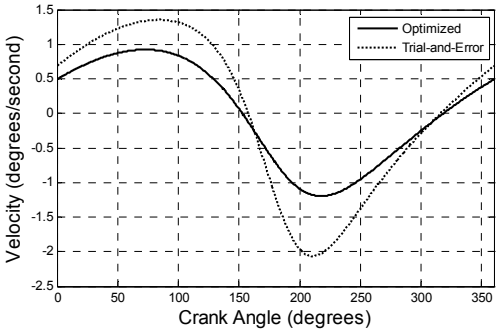

Figure 5.14: Velocity of Link Z_{10} vs. Crank Angle

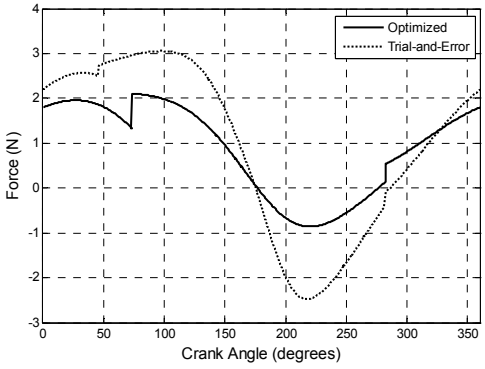

Figure 5.15: X-Direction of Force Between Link 1 and Link 2 vs. Crank Angle

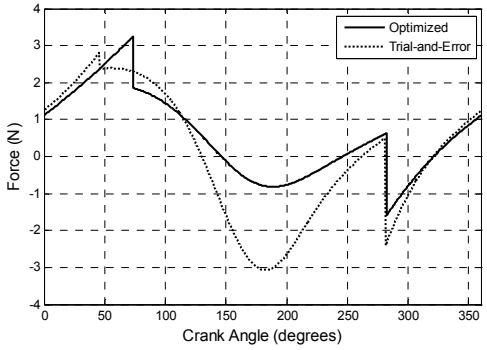

Figure 5.16: Y-Direction of Force Between Link 1 and Link 2 vs. Crank Angle

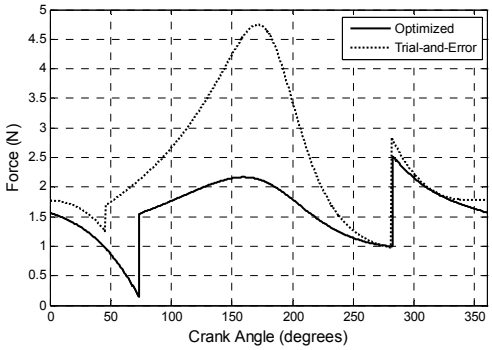

Figure 5.17: X-Direction of Force Between Link 2 and Link 3 vs. Crank Angle

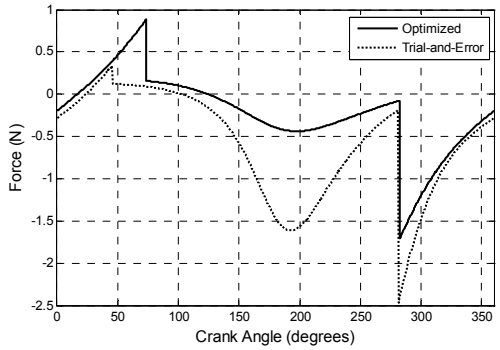

Figure 5.18: Y-Direction of Force Between Link 2 and Link 3 vs. Crank Angle

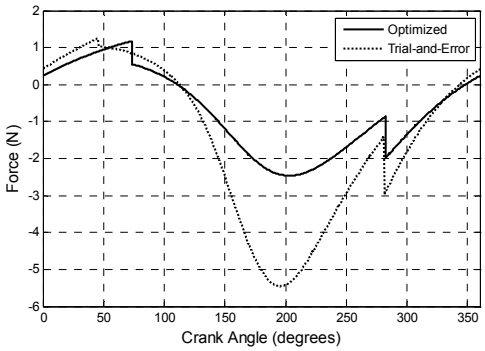

Figure 5.19: X-Direction of Force Between Link 2 and Link 5 vs. Crank Angle

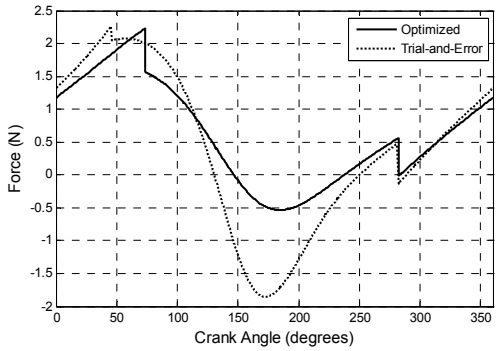

Figure 5.20: Y-Direction of Force Between Link 2 and Link 5 vs. Crank Angle

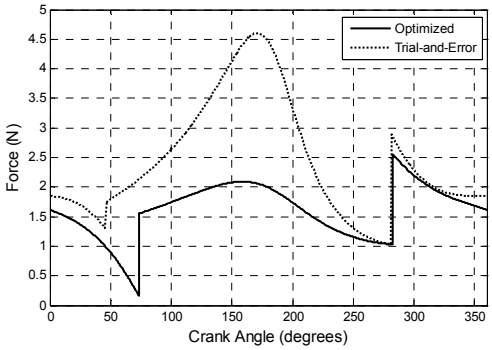

Figure 5.21: X-Direction of Force Between Link 3 and Link 4 vs. Crank Angle

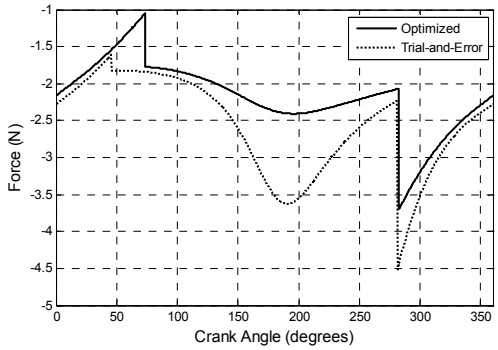

Figure 5.22: Y-Direction of Force Between Link 3 and Link 4 vs. Crank Angle

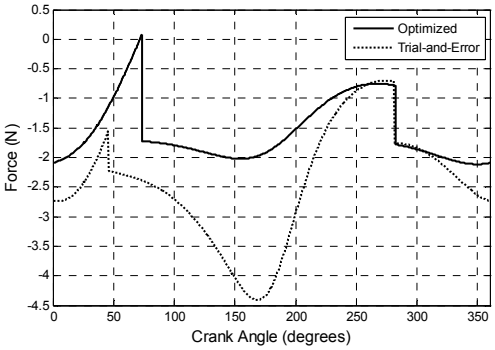

Figure 5.23: X-Direction of Force Between Link 1 and Link 4 vs. Crank Angle

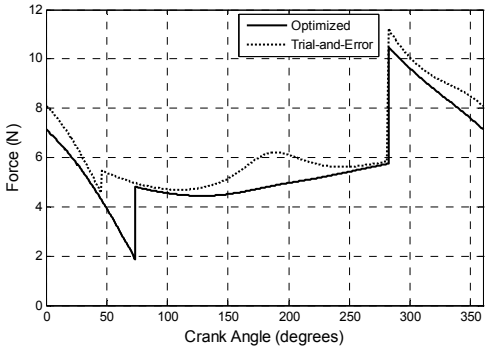

Figure 5.24: Y-Direction of Force Between Link 1 and Link 4 vs. Crank Angle

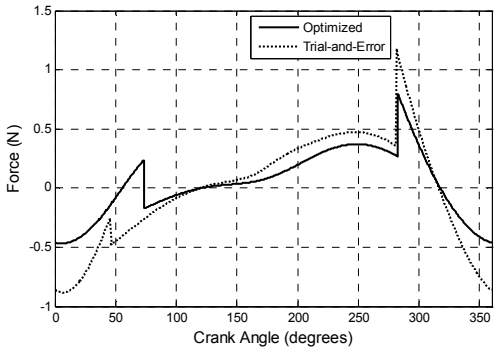

Figure 5.25: X-Direction of Force Between Link 4 and Link 9 vs. Crank Angle

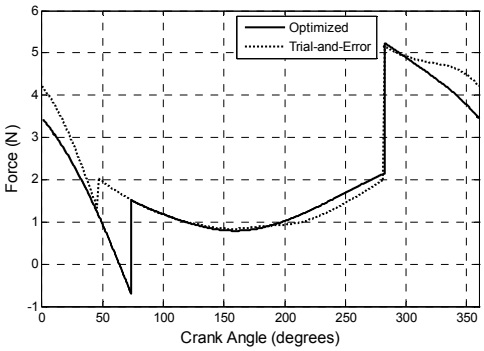

Figure 5.26: Y-Direction of Force Between Link 4 and Link 9 vs. Crank Angle

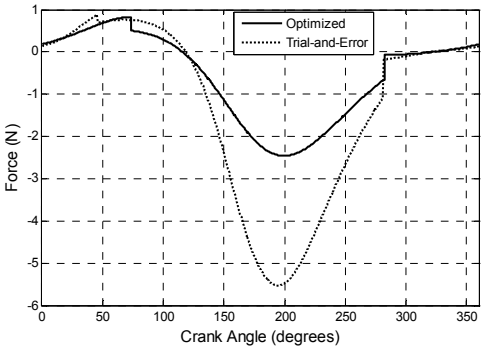

Figure 5.27: X-Direction of Force Between Link 5 and Link 6 vs. Crank Angle

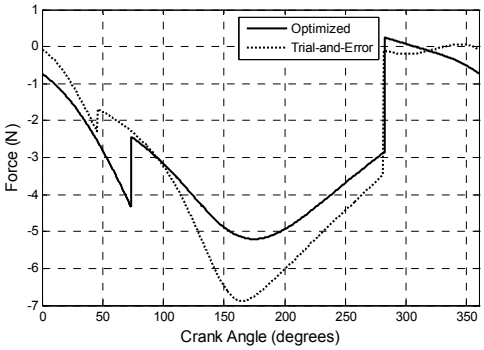

Figure 5.28: Y-Direction of Force Between Link 5 and Link 6 vs. Crank Angle

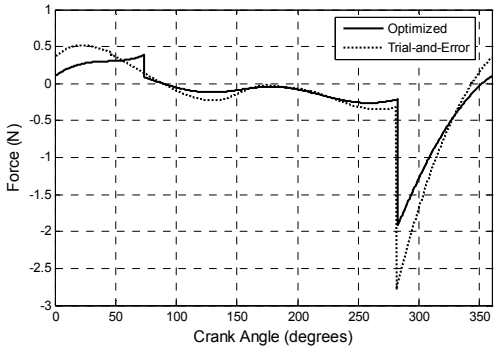

Figure 5.29: X-Direction of Force Between Link 5 and Link 10 vs. Crank Angle

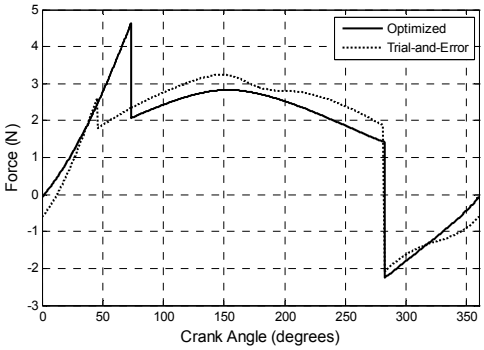

Figure 5.30: Y-Direction of Force Between Link 5 and Link 10 vs. Crank Angle

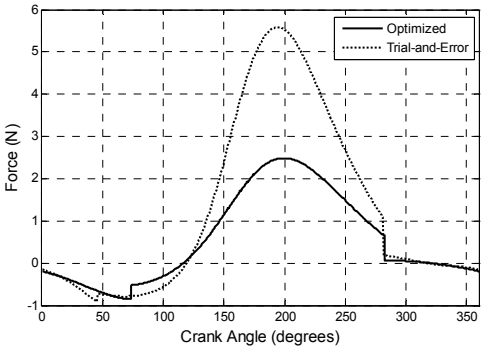

Figure 5.31: X-Direction of Force Between Link 1 and Link 6 vs. Crank Angle

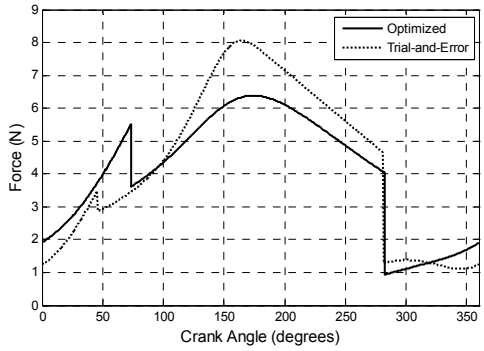

Figure 5.32: Y-Direction of Force Between Link 1 and Link 6 vs. Crank Angle

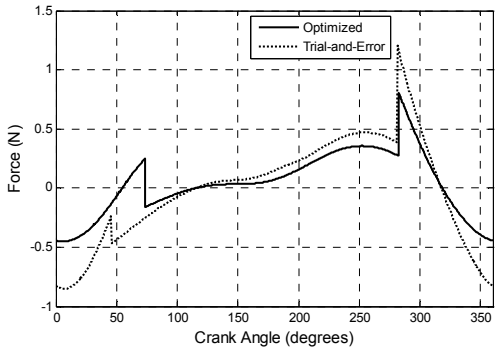

Figure 5.33: X-Direction of Force Between Link 9 and Link 10 vs. Crank Angle

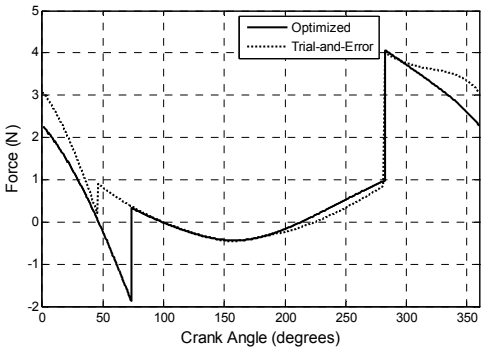

Figure 5.34: Y-Direction of Force Between Link 9 and Link 10 vs. Crank Angle

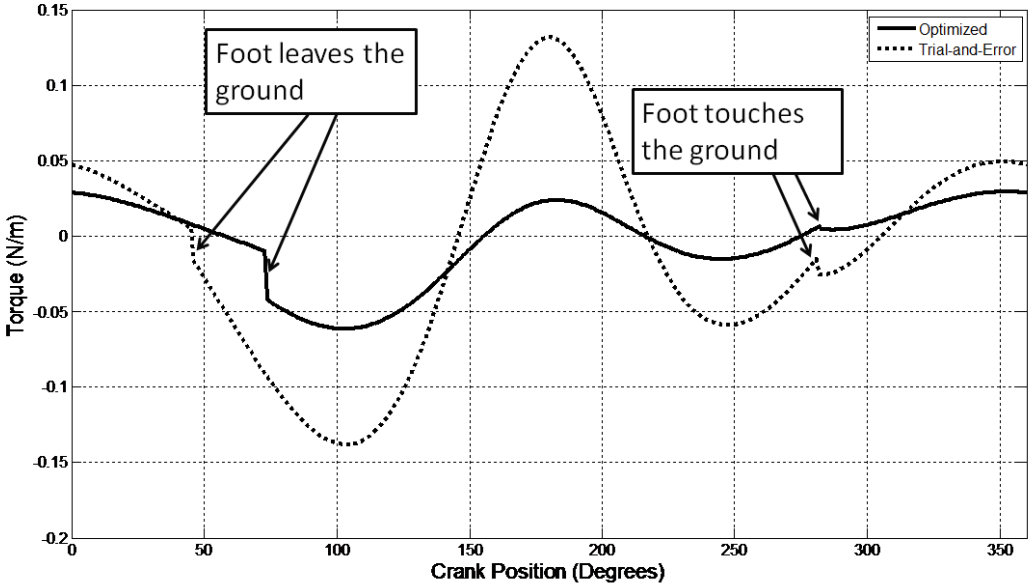

Figure 5.35: Torque Curves

5.5 Physical Prototype

To examine the success of the research, a low-cost physical prototype (Figure 5.36) was built to examine if its behaviour and performance match the computer model. Unfortunately with this simple prototype the forces acting at the feet are not measured, however its motion can be video recorded as well as general observations of its performance. The links and the majority of the frame are made of ¾ inch EMT (electrical metal conduit) metal tubing. Holes were drilled into the ends of the links and a 3/16 inch

metal rod was inserted and used to create the joints between the links; except for the links attached to the frame because they have a connector glued on the end which slides over the tubing. Angle and flat steel with pre drilled holes are used at each end to create a frame that can easily attach casters for mild support of the structure. The castors are also made adjustable to control the magnitude of support. A DC motor with a gear reduction and a variable speed control is attached at each end of the crank. The motors are reversible which allows the mechanism to walk in both directions. Each leg pairing is comprised of 22 links. In total there are three pairs of legs and a total of 66 links. To try and space the leg pairings evenly apart, the crank of each pair is offset by 120° to try and have consistent motion when being propelled forward. To increase friction between the feet and the ground, rubber was added at the foot. This also adds some cushioning between the foot and the ground to reduce impact. Furthermore, the lengths of the legs were chosen to be scaled 1.4 times than the optimized dimensions listed in Table 5.1.

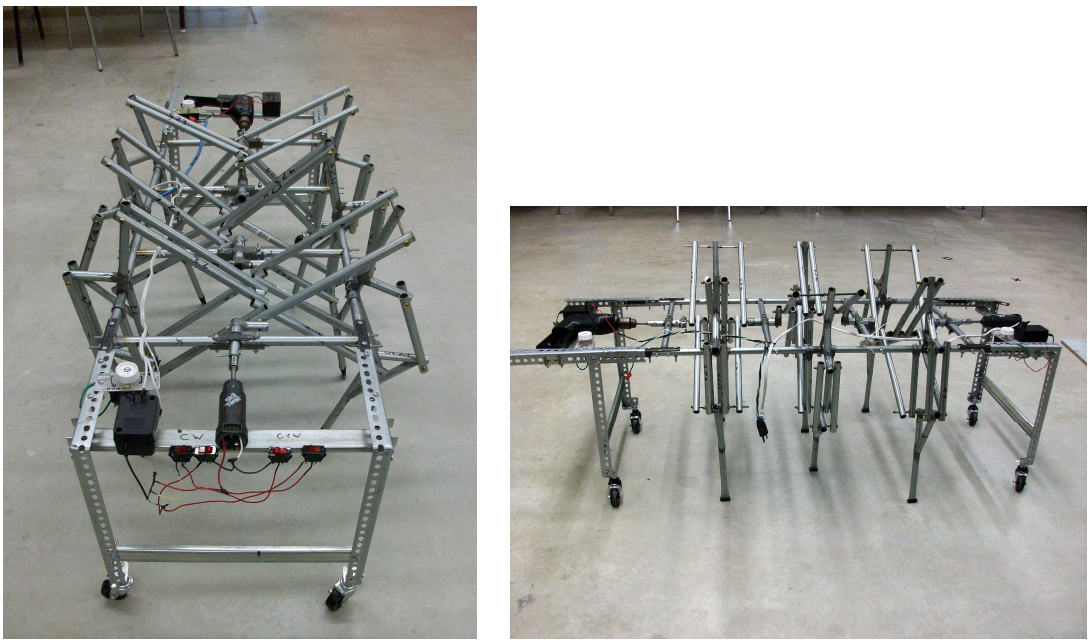

Figure 5.36: Physical Prototype of the Leg Mechanism

The mechanism's overall dimensions are 149.9 cm long, by 66.0 cm wide and 64.8 cm high. Figure 5.37 shows progressive shots of a single leg moving. From the figure it can be seen that the motion of the foot performs similar to that of the computer model, thus justifying that the model is accurate when compared to reality. Figure 5.38 shows a progressive still shot of the entire mechanism moving which indicates that the prototype does function and works correctly.

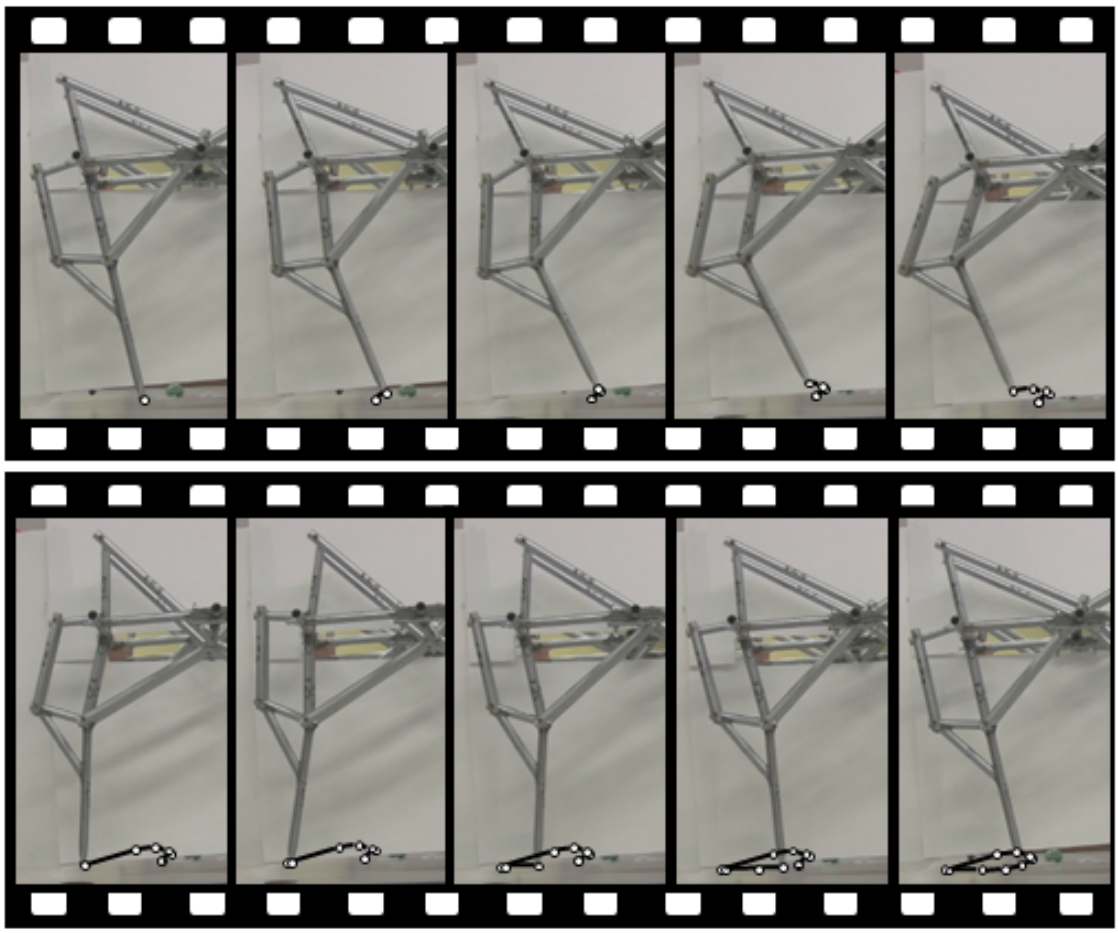

Figure 5.37: Progressive Still Shot of a Single Leg Motion

After building the prototype certain problems and areas of improvement were found. Some of the problems are caused by the low precision used to build the prototype. One

area of concern is the crank that drives the system. The crank that drives each pair of legs is comprised of two links. The problem occurs because one of the crank links can lag slightly due to the low tolerances in the joint. This causes the joint to bind causing a significant increase in torque. To overcome this, the crank links can be welded to the joint rod connecting the two. However, this creates a problem when removing any of the links. Another way is to flatten the one end of the links that attach to the crank, because then the length of the crank pin is shortened which would aid in reducing the significance of the binding. One last method is to reconstruct a new prototype. One way is to design a model that utilizes tight tolerances, bearings in the joints, and a solid crank. This was undesirable for the first prototype because the cost would increase substantially with machining costs, bearings, labour costs and higher quality materials. Another way is to fabricate them by using the methods described by Theo Jansen [28]. Even though the materials used by Theo Jansen are very cheap, he does mention in his book [28] that he required specific tools to construct these mechanisms. It would be feasible to acquire such tools if many mechanisms were going to be built, however for just a few it becomes very unfeasible.

5.6 Summary

An optimization was applied to the leg mechanism to improve on the leg performance. The objective problem that describes the optimization is composed of two components: i) reduction of energy and ii) maximizing the step length. The results were then compared to a previously achieved trial-and-error solution.

It was found that there were large improvements on the overall objective function. This improvement was directly related to the reduction in energy because the performance in the step length decreased. However, the magnitude at which the step length decreased is not substantial. To demonstrate the optimized solution, a physical prototype was constructed to show that it works and that it behaves in a manner that was depicted by the computer model.

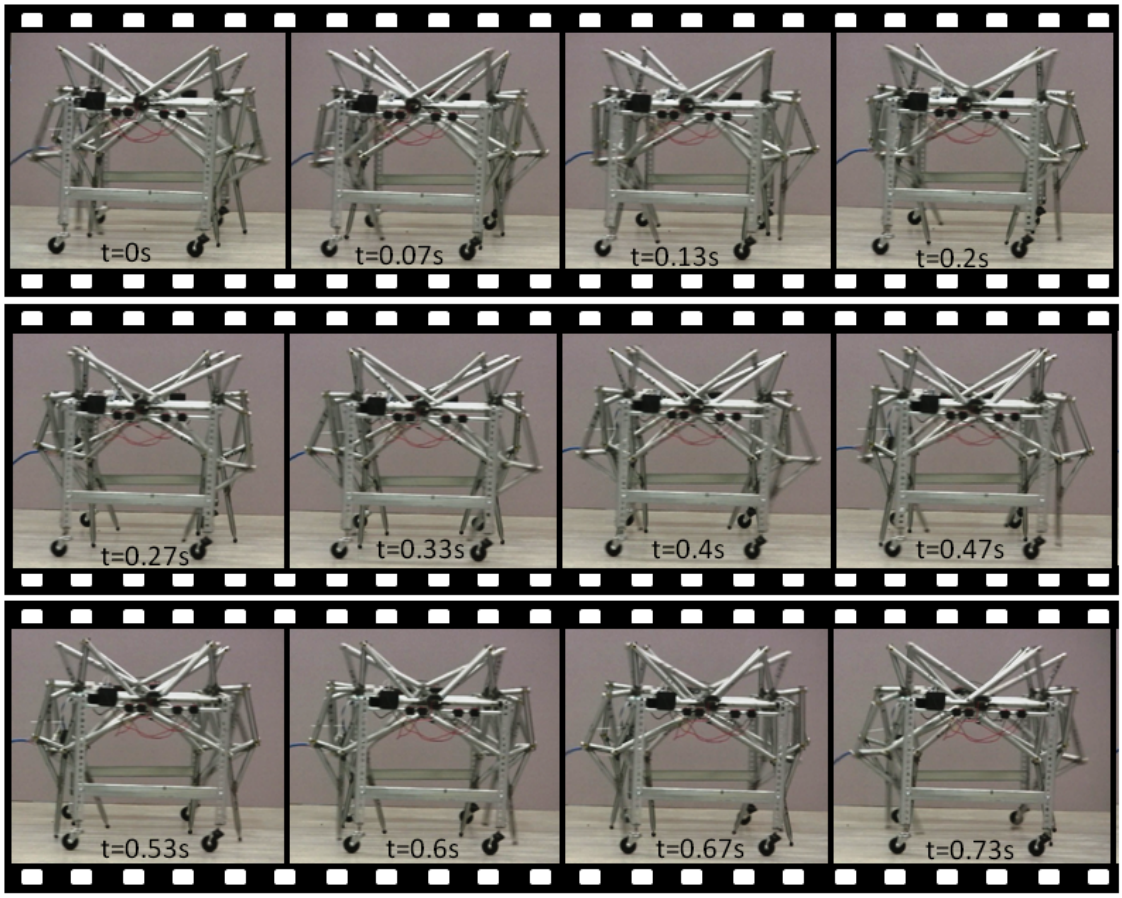

Figure 5.38: Progressive Still Shot of the Leg's Motion

Chapter 6

6. Conclusion and Future Work

6.1 Conclusions

A SDOF leg mechanism used by Theo Jansen was redesigned using mechanism design theory for the purposes of optimization. The optimization of the leg mechanism required the following studies to be performed: a) the design of the leg using mechanism design, b) an initial study on improving the mechanism using trial-and-error c) the complete kinematic derivation describing each link, d) the complete derivation of the dynamics of each link and e) the creation of the objective functions representing the desired goals of the optimization.

The design of the leg mechanism was separated into two main design stages. The first is the design of the two identical four-bar mechanisms ($Z_1Z_2Z_3Z_4$ and $Z_1Z_2Z_5Z_6$, Figure 2.2) and the coupler $Z_4Z_7Z_8$. The four-bar mechanisms were treated as a function generator and were designed based on an equation describing their motion. The coupler was designed by free choices defined by the user. The second design stage is the design of the $Z_6Z_8Z_9Z_{10}Z_{11}Z_{12}$ (Figure 2.2) mechanism, this mechanism was treated as a path generator. The design was carried out using four precision point synthesis where the path was specified by the user. After the design was complete, constraints were formulated to aid in determining if the designed mechanism was acceptable. With the use of these

methods a trial-and-error manual optimization was performed. The parameters needed to design the leg were manually chosen and changed by the user until an excellent looking mechanism was found.

To perform the optimization a complete analysis of the leg mechanism was needed. Kinematics was the first analysis since the dynamics are dependent on the solved kinematics. The kinematics was solved by separating the leg mechanism into three loops. With the use of the loop closure equations the angle, velocity and acceleration was found for each link. Since the leg is a SDOF, the kinematics of one link needed to be defined to solve for the remaining. With the derivations of the kinematics, the dynamics of the leg mechanism can be solved.

The dynamics were derived by analysing each link separately by creating a force diagram depicting all the forces acting on the link's body, including inertia forces. As a result three equations were derived for each link. Two are obtained by summing the forces on the body and separating them into their respective x and y-components. The third was derived by summing the moments about the center of mass. As a result, 21 linear equations were found and with the use of superposition these equations form a matrix representing the dynamics of the system. However, 23 unknowns were found in the system making it redundant to solve. Therefore, assumptions had to be made concerning the ground reaction forces between the foot and the ground, which is a common occurrence in previous research.

The last and sometimes the most critical step in terms of optimizations are the objective functions. For this problem, two critical aspects of the leg mechanisms performance were

chosen to be optimized. First, is minimizing the energy to improve the efficiency of the leg and lowering the requirement for larger motors. Second, is the maximization of the stride length, because a leg that travels a longer distance with lower energy is very desirable. Hence, I want to reduce the amount of energy per unit of travel.

The optimization was performed using Matlab's optimization toolbox. However, it was found that many local minimums exist, therefore a coarse exhaustive search was performed where the optimization was applied to the best found configurations. The results of this thesis show that a large increase in the performance of the leg mechanism was found. Therefore, the optimization was a success. However, the goals of this work was not only the optimization, but to show that mechanism design should be considered for optimizations of a leg mechanism, because they offer more control over the outcome of each solution and eliminates the analysis of impossible mechanisms that would otherwise be analysed. In previous studies, the link lengths were changed directly [12,14,18,19], thus blindly changing the lengths in hopes that the new configuration will be valid and have better performance. With the mechanism design theory, the chances that the new configuration is valid greatly increases since it must satisfy certain precision points defining the foot path.

The comparison between the trial-and-error and optimization results demonstrates an excellent improvement in the performance of the mechanism. The mechanism design theory was found to be an excellent tool for determining the link lengths when incorporated into the optimization, because it offers a greater control on the outcome of each solution. The dynamic analysis was utilized in the optimization process to better simulate the forces in the joints and the torque on the crank. However, the dynamics is

highly dependent on the assumptions and would need to be tested to increase the confidence of the dynamic analysis model. Overall, with the combination of the mechanism design and the dynamics, a very successful optimization was created where the energy and maximum crank torque were reduced drastically.

6.2 Future Work

Even though the optimization was a success, there was a critical assumption made regarding the reaction forces seen at the foot. This is a common problem in previous research as well [11,12,14,19]. However, the actual forces experienced at the foot have not been studied. This could be due to the fact that previous work utilized the static force analysis techniques instead of dynamics. As a result, it is being planned to test the prototype of the leg mechanism with the intentions to physically measure the reaction forces at the foot. The measured data would then be compared to the ground reaction assumptions to examine its resemblance to the measured data. Then by examining these differences it is desirable to try and better simulate reality by adjusting these assumptions.

References:

[1] Bekker, M.G., *"Off-the-Road Locomotion"*, University of Michigan Press, Ann Arbor, MI (1960).

[2] Uglow, Jenny, *The Lunar Men*, London: Faber and Faber, 2002.

[3] Mosher, R. S., "Testing and Evaluation of a Versitile Walking Truck," *In Proceeding of the Off-Road Mobility Research Symposium*. Int. Soc. For Terrain Vehicle Systems, 1968, pp. 12.

[4] Reeve. R, *Generating Walking Behaviours in Legged Robots*, Ph.D. Thesis: University of Edinburgh, 1999.

[5] *STIC Insect by Univ of S. Queensland, Australia.* [cited 2010, March 8], Available HTTP: http://www.arrickrobotics.com/robomenu/stic.html

[6] *Spring Walker*. [cited 2010, March 8], Available HTTP: http://www.springwalker.com/

[7] MIT Leg Lab, *Milestones in the Development of Legged Robots*. [cited 2010, March 8], Available HTTP: http://www.ai.mit.edu/projects/leglab/background/milestones.html

[8] Funabashi, H., Ogawa, K., Gotoh, Y., Kojima, F., "Synthesis of Leg-Mechanisms of Biped Walking Machines (Part I, Synthesis of Ankle-Path-Generator)," *Bulletin of the JSME*, vol. 28, no. 237, pp. 537-543, Mar. 1985.

[9] Todd, D.J., " Evaluation of Mechanically Co-ordinated Legged Locomotion (The Iron Mule Train revisited)," *Robotica*, vol. 9, no. pt 4, pp. 417-420, Oct-Dec 1991.

[10] Funabashi, H., Ogawa, K., Honda, I., Iwatsuki, N., " Synthesis of Leg-Mechanisms of Biped Walking Machines (Part II, Synthesis of Foot-Driving Mechanism)," *Bulletin of the JSME*, vol. 28, no. 237, pp. 544-549, Mar 1985.

[11] Williams, R.P., Tsai, L.W. and Azarm, S., "Design of a Crank-and-Rocker Driven Pantograph: A Leg Mechanism for the University of Maryland's 1991 Walking Robot", *Proc. Of 2nd Nat. Conf. On Applied Mechanisms and Robotics,* **1**, Paper No. VIB.2, Cincinnati, OH, 1991.

[12] Shieh, W.-B., Tsai, L.-W., Azarm, S., " Design and Optimization of a One-Degree-of-Freedom Six-Bar Leg Mechanism for a Walking Machine," *Journal of Robotic Systems*, vol. 14, no. 12, pp. 871-880, Dec. 1997.

[13] *Strandbeest*. [cited 2010, March 8], Available HTTP: www.strandbeest.com

[14] Shieh, W.-B., Tsai, L.-W., Azarm, S., Tits, A.L., "Optimization-Based Design of a Leg Mechanism Via Combined Kinematic and Structural Analysis," *American Society of Mechanical Engineers, Design Engineering Division (Publication) DE*, vol. 69-1, pp. 199-209, 1994.

[15] Song, S., Waldron, K. J., *Machines That Walk: The Adaptive Suspension Vehicle*, Cambridge: MIT Press, 1990.

[16] Moreckie, A.A., Bianchi, G. And Kedzior, K., “Theory and Practice of Robots and Manipulators,” *Proc. of Romansy 1984: The fifth CISM-IFToMM Symposium*, p. 403, Kogan Page, London. Hermes Publishing, 1985.

[17] Pugh, D., Ribble, E. Vohnout, V. Bihari, T., Walliser, T., Patterson, M. And Waldron, K., “Technical Description of the Adaptive Suspension Vehicle,” *The International Journal of Robotics Research*, Vol. 9, No. 2, pp. 24-42 (1990)

[18] Song, S.-M., Waldron, K.J., Kinzel, G.L., "Computer-Aided Geometric Design of Legs for a Walking Vehicle," *Mechanism and Machine Theory*, vol. 20, no. 6, pp. 587-596, 1985.

[19] Shieh, W.-B., Tsai, L.-W., Azarm, S., Tits, A.L., " Multiobjective Optimization of a Leg Mechanism with Various Spring Configurations for Force Reduction," *Journal of Mechanical Design, Transactions of the ASME*, vol. 118, no. 2, pp. 179-185, Jun 1996.

[20] Uicker Jr, J. J., Pennock, G. R., Shigley, J. E., *Theory of Machines and Mechanisms*, Third ed. , New York, New York: Oxford University Press, Inc., 2003.

[21] Waldron, K. J., Kinzel, G. L., *Kinematics, Dynamics, and Design of Machinery*, New York, New York: John Wiley and Sons, Inc., 1999.

[22] Erdman, A. G., Sandor, G. N., *Mechanism Design: Analysis and Synthesis Vol. 1*, Third ed., Upper Saddle River, New Jersey: Prentice-Hall, Inc., 1997.

[23] Singh, V.P., Sharma, S., Thakur, B.S., " Kinematic synthesis and optimization of four-bar linkage," *Journal of the Institution of Engineers (India): Mechanical Engineering Division*, vol. 85, no. Jan, pp. 199-205, 2005.

[24] Erdman, A. G., Sandor, G. N., *Advanced Mechanism Design: Analysis and Synthesis Vol. II*, Englewood Cliffs, New Jersey: Prentice-Hall, Inc., 1984.

[25] Myszka, D. H., *Machines & Mechanisms: Applied Kinematic Analysis*, Third ed., Saddle River, New Jersey: Prentice-Hall, Inc., 2005.

[26] Cleghorn, W.L., *Mechanics of Machines*, New York, New York: Oxford University Press, Inc., 2005.

[27] Andersson, J., "A Survey of Multiobjective Optimization in Engineering Design," *Technical Report: LiTH-IKP-R-1097*. Department of Mechanical Engineering, Linköping University, 581 83 Linköping, Sweden.

[28] Jansen, T., *The Great Pretender*, Rotterdam: 010 Publishers, 2007.